The role of miR-21 in the pathophysiology of neuropathic pain using the model of B7-H1 knockout mice

Die Rolle von miR-21 in der Pathophysiologie von neuropathischem Schmerz am Model der B7-H1 defizienten Maus

Doctoral thesis for a doctoral degree

at the Graduate School of Life Sciences,

Julius-Maximilians-Universität Würzburg,

Section Neuroscience

submitted by

Franziska Karl

from

Werneck

Würzburg 2017

Submitted on:

……..……..

Office stamp

Members of the Promotionskomitee:

Chairperson: Prof. Dr. Ulrike Holzgrabe

Primary Supervisor: Prof. Dr. Claudia Sommer

Supervisor (Second): Prof. Dr. Thomas Dandekar

Supervisor (Third): Dr. Ana Eulalio

Supervisor (Fourth): Prof. Dr. Nurcan Üçeyler

Date of Public Defence: ……..……

Date of Receipt of Certificates:

……

Affidavit

I hereby confirm that my thesis entitled “The role of miR-21 in the pathophysiology of neuropathic pain using the model of B7-H1 knockout mice” is the result of my own work. I did not receive any help or support from commercial consultants. All sources and / or materials applied are listed and specified in the thesis.

Furthermore, I confirm that the thesis has not yet been submitted as part of another examination process neither in identical nor in similar form.

Place, Date Signature

Eidesstattliche Erklärung

Hiermit erkläre ich an Eides statt, die Dissertation „Die Rolle von miR-21 in der Pathophysiologie von neuropathischem Schmerz am Model der B7-H1 defizienten Maus“ eigenständig, d.h. insbesondere selbstständig und ohne Hilfe eines kommerziellen Promotionsberaters, angefertigt und keine anderen, als die von mir angegebenen Quellen und Hilfsmittel verwendet zu haben.

Ich erkläre außerdem, dass die Dissertation weder in gleicher noch in ähnlicher Form bereits in einem anderen Prüfungsverfahren vorgelegen hat.

Ort, Datum Unterschrift

Parts of the results presented in this thesis have been published:

Karl F, Grießhammer A, Üçeyler N and Sommer C (2017) Differential impact of miR-21 on pain and associated affective and cognitive behavior after spared nerve injury in B7-H1 ko mouse. Front Mol Neurosci. 10:219. doi: 10.3389/fnmol.2017.00219.

The published manuscript and this thesis contain similar text passages in adapted form in some sections.

1 Abstract

The impact of microRNA (miRNA) as key players in the regulation of immune and neuronal gene expression and their role as master switches in the pathophysiology of neuropathic pain is increasingly recognized. miR-21 is a promising candidate that could be linked to the immune and the nociceptive system. To further investigate the pathophysiological role of miR-21 in neuropathic pain, we assesed mice deficient of B7 homolog 1 (B7-H1 ko), a protein with suppressive effect on inflammatory responses.

B7-H1 ko mice and wildtype littermates (WT) of three different age-groups, young (8 weeks), middle-aged (6 months), and old (12 months) received a spared nerve injury (SNI). Thermal withdrawal latencies and mechanical withdrawal thresholds were determined. Further, we investigated anxiety-, depression-like and cognitive behavior. Quantitative real time PCR was used to determine miR-21 relative expression in peripheral nerves, dorsal root ganglia and white blood cells (WBC) at distinct time points after SNI.

Naïve B7-H1 ko mice showed mechanical hyposensitivity with increasing age. Young and middle-aged B7-H1 ko mice displayed lower mechanical withdrawal thresholds compared to WT mice. From day three after SNI both genotypes developed mechanical and heat hypersensitivity, without intergroup differences. As supported by the results of three behavioral tests, no relevant differences were found for anxiety-like behavior after SNI in B7-H1 ko and WT mice. Also, there was no indication of depression-like behavior after SNI or any effect of SNI on cognition in both genotypes. The injured nerves of B7-H1 ko and WT mice showed higher miR-21 expression and invasion of macrophages and T cells 7 days after SNI without intergroup differences. Perineurial miR-21 inhibitor injection reversed SNI-induced mechanical and heat hypersensitivity in old B7-H1 ko and WT mice.

This study reveals that reduced mechanical thresholds and heat withdrawal latencies are associated with miR-21 induction in the tibial and common peroneal nerve after SNI, which can be reversed by perineurial injection of a miR-21 inhibitor. Contrary to expectations, miR-21 expression levels were not higher in B7-H1 ko compared to WT mice. Thus, the B7-H1 ko mouse may be of minor importance for the study of miR-21 related pain. However, these results spot the contribution of miR-21 in the

pathophysiology of neuropathic pain and emphasize the crucial role of miRNA in the regulation of neuronal and immune circuits that contribute to neuropathic pain.

2 Zusammenfassung

Die Beteiligung von microRNA (miRNA) an der Genregulation immunologischer und neuronaler Prozesse und deren Rolle als Schlüsselelement in der Pathophysiologie von neuropathischem Schmerz gewinnt zunehmend an Bedeutung. miR-21 ist ein vielversprechender Kandidat, der sowohl das Immunsystem, als auch das nozizeptive System beeinflusst. Um die pathophysiologische Rolle von miR-21 bei neuropathischem Schmerz besser zu verstehen wurden Mäuse mit B7 homolog 1 Defizienz (B7-H1 ko), einem immunsupprimierendem Protein, untersucht. Eine frühere Studie zeigte eine Hochregulierung von miR-21 in murinen Lymphozyten.

Junge (8 Wochen), mittelalte (6 Monate) und alte (12 Monate) B7-H1 ko Mäuse und Wildtypwurfgeschwister (WT) erhielten eine spared nerve injury (SNI) als neuropathischem Schmerzmodell. Es wurden thermische Rückzugslatenzen und mechanische Rückzugsschwellen bestimmt. Des weiteren wurde sowohl das Angstverhalten, das depressive Verhalten, als auch das kognitive Verhalten untersucht. Um die relative Expression von miR-21 in den peripheren Nerven, den Spinalganglien und in den weißen Blutzellen zu verschiedenen Zeitpunkten zu bestimmen, wurde die quantitative real time PCR angewandt.

Naive B7-H1 ko Mäuse zeigten mit zunehmendem Alter eine mechanische Hyposensitivität. Bereits 3 Tage nach SNI entwickelten beide Genotypen eine Überempfindlichkeit gegenüber Hitze und mechanischer Stimulation. In drei durchgeführten Verhaltenstests konnten keine relevanten Unterschiede im Angstverhalten nach SNI von B7-H1 ko und WT Mäusen festgestellt werden. Bei beiden Genotypen gab es weder Hinweise auf depressives Verhalten nach SNI, noch wurde das kognitive Verhalten durch SNI beeinträchtigt. Die verletzen Nerven der B7-H1 ko und WT Mäuse zeigten 7 Tage nach SNI eine höhere miR-21 Expression und eine Invasion durch Makrophagen und T-Zellen ohne Gruppenunterschiede. Die perineurale Injektion eines miR-21 Inhibitors konnte die durch SNI induzierte mechanische und thermische Hypersensitivität lindern.

Diese Studie zeigt, dass der Anstieg von miR-21 im N. tibialis und N. peroneus communis mit reduzierten Rückzugsschwellen gegen mechanische Reize und verkürzten Wegzugslatenzen bei Hitzestimulation einhergeht, welche durch perineurale Injektion eines miR-21 Inhibitors verringert werden können. Entgegen der Erwartungen zeigten B7-H1 ko Mäuse im Vergleich zu WT Mäusen keine erhöhte

miR-21 Expression und sind daher möglicherweise von geringer Bedeutung für die Untersuchung von miR-21 assoziiertem Schmerz. Jedoch bekräftigen diese Ergebnisse eine Beteiligung von miR-21 an der Pathophysiologie von neuropathischem Schmerz und bestätigen die wichtige Rolle von miRNA bei der Regulation von neuronalen und immunologischen Prozessen, die zu neuropathischem Schmerz beitragen.

3 Introduction

3.1 Pain and nociception

Pain is an acute warning system of the body and necessary to ensure survival and health. The response of the sensory nervous system to stimuli that might cause tissue damage is called nociception. Nociceptive stimuli (mechanical, thermal or chemical) are translated into electric impulses and conducted by primary afferent peripheral nerve fibers, called nociceptors (Basbaum et al., 2009). The cell bodies of nociceptors are located in the dorsal root ganglia (DRG) and trigeminal ganglia with their peripheral axon innervating the target organ and the proximal axon connecting to the dorsal horn of the spinal cord. From here, incoming action potentials are projected to the brain, where pain is perceived (Figure 1). Primary afferent peripheral nerve fibers can be categorized into three different groups. The Aβ nerve fibers are large diameter, myelinated, and fast conducting fibers, and are responsible for the detection of light touch. Most of the nociceptors belong to the Aδ and C nerve fibers. Aδ fibers are of medium diameter and thinly myelinated axons with a conduction velocity of 6-25 m/s, while C fibers, with the smallest diameter and without myelination, have a slower conduction velocity (1 m/s). Aδ fibers mediate the acute, “first” or fast pain, whereas C fibers are responsible for the so called “second” or slow pain (Julius and Basbaum, 2001;Kuner and Flor, 2016). In electrophysiological studies two main classes of Aδ nociceptors were identified. The type 1 high-threshold mechanical nociceptors respond to intensive mechanical and heat stimuli, with high heat thresholds over 50˚C. In case of tissue injury, these fibers are sensitized dropping the perception thresholds. Type 2 Aδ nociceptors have lower heat thresholds, but higher mechanical thresholds (Basbaum et al., 2009). C fibers respond to thermal, mechanical, and chemical stimuli, like histamine or capsaicin. The so called silent nociceptors are unmyelinated afferents, which respond to heat and chemical stimuli and also to mechanical stimuli, however, only in case of tissue damage (Namer et al., 2015).

C fibers can further be classified by their molecular properties. The peptidergic population of C nociceptors release neuropeptides, substance P, and calcitonin-gene related peptide (CGRP) and express tropomyosin receptor kinase A (TrkA), the high-affinity tyrosine kinase receptor for nerve growth factor (NGF) (Snider and McMahon, 1998). The second, non-peptidergic class of C fibers shows distinct properties like

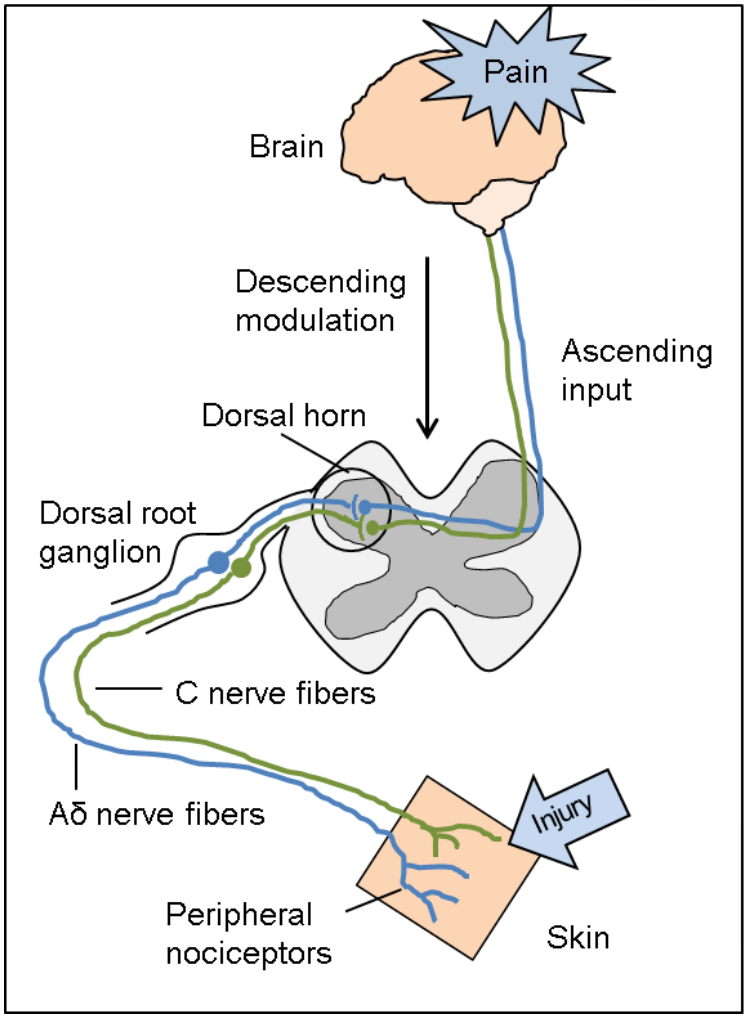

Figure 1: Illustration of the nociceptive pathway. Peripheral nociceptors, Aδ and C fibers, respond to noxious stimuli by transducing signals to the spinal cord. From the dorsal root ganglia, the primary nociceptive neurons enter the spinal cord through the ipsilateral dorsal horn, where secondary neurons cross to the contralateral side via the anterior commissure, and ascend to the brain.

the expression of the c-Ret neutrophin receptor, which is targeted by glial-derived neurotrophic factor (GDNF). Most of these nociceptors also have binding sites for IB4 (Dong et al., 2001). Providing evidence for distinct subtypes of C-fibers, a recent study identified three classes of itch responsive type C neurons with unique response profiles and markedly different molecular properties, like histamine and serotonin receptors (Usoskin et al., 2015).

Nociceptive afferents transduce signals to second-order neurons in the spinal dorsal horn (mostly laminae I and II), from where input is projected to the lateral thalamic nuclei (lateral spinothalamic tract) or to the brainstem (spinoreticulothamalic tract). From the thalamus, neurons project towards the somatosensory cortex, where pain is perceived. Other neurons project from the brainstem and amygdala to the cingulate and insular cortices, where emotional and affective components of pain are further processed (Kuner, 2010). Descending pathways from the brain send information to the spinal cord to enable withdrawal from the noxious stimuli.

3.2 Neuropathic pain

Besides its warning and protective function, pain can occur spontaneously or may be evoked by normally innocuous stimuli. According to the International Association for

the Study of Pain (IASP) neuropathic pain is defined as “pain arising as a direct consequence of a lesion or disease affecting the somatosensory system” (Treede et al., 2008). Neuropathic pain can be caused by acquired or genetic diseases or lesions of the central and peripheral nervous system. Examples are metabolic, infectious, and autoimmune disorders, as well as toxic and traumatic lesions. Neuropathic pain may be accompanied by paradoxical sensory perceptions and can be associated with “negative” symptoms, such as numbness and hypoesthesia, as well as with “positive” symptoms such as allodynia (pain triggered by a stimulus that normally does not evoke pain) and hyperalgesia (an increased pain response produced by a stimulus that normally causes pain) (Jensen and Finnerup, 2014). Neuropathic pain, which affects about 7-10 % of the population (Bouhassira et al., 2008;Jensen and Finnerup, 2014;van Hecke et al., 2014), substantially impairs everyday life activities and reduces working performance and patients’ health related quality of life (Blyth et al., 2003). Furthermore, neuropathic pain has an emotional component and is frequently associated with depression and anxiety (Jain et al., 2011). Epidemiological studies report a mean prevalence of about 30 % for developing depressive disorders in patients with neuropathic pain (Gustorff et al., 2008;Attal et al., 2011). The diagnosis is made following national and international guidelines (Colloca et al., 2017). Due to the heterogeneity of neuropathic pain mechanisms, analgesic treatment remains difficult and current treatment strategies, which are mainly based on symptoms rather than on mechanisms, do not always lead to sufficient pain relief (Baron et al., 2010).

3.2.1 Animal models of neuropathic pain

Most of the knowledge about mechanisms of neuropathic pain is based on preclinical studies from animal models and in vitro experiments. Various animal models have been developed to induce neuropathic pain and investigate the underlying pathomechanisms. Rodent models of neuropathic pain can be based e.g. on cancer pain, drug-induced pain, metabolic neuropathies, and peripheral nerve injuries (Jaggi et al., 2011;Yalcin et al., 2014). Most of the peripheral nerve lesion models make use of partial or complete lesions of the sciatic nerve. The common principle of these models is the induction of mechanical and/or thermal hypersensitivity and spontaneous pain associated behavior. One example is the chronic constrictive injury (CCI) model that is based on several loose ligatures placed around the main branch of the sciatic nerve (Bennett and Xie, 1988). This leads to spontaneous pain, thermal,

and mechanical hyperalgesia and lasts for over two months. In the partial sciatic nerve ligation (PSL) model a hemi-ligation of the sciatic nerve is performed that induces mechanical and thermal hypersensitivity over seven months (Seltzer et al., 1990), whereas for L5/L6 spinal nerve ligation (SNL) the L5 and L6 spinal nerves are tightly ligated, which is associated with pain behavior for at least four months (Kim and Chung, 1992). Another model is the spared nerve injury (SNI) applying a ligature around the tibial and common peroneal nerves with consecutive distal axotomy (Decosterd and Woolf, 2000). SNI leads to long lasting (> 6 months), increased mechanical sensitivity and thermal responsiveness in the sural territory of the hind paw and was also used in our study (see below).

3.2.2 Pathophysiology of neuropathic pain

Modulations in the central nervous system (CNS), like central sensitization in the postsynaptic dorsal horn is caused by synaptic plasticity and lead to increased descending response (Woolf, 2011). Especially ongoing discharge of peripheral afferent fibers results in the release of excitatory amino acids and neuropeptides, which leads to postsynaptic changes in second-order nociceptive neurons, like phosphorylation of N-methyl-D-aspartate (NMDA) receptors and α-amino-3-hydroxy-5-methyl-4-isoxazolepropionic acid (AMPA) receptors (Baron et al., 2013). In the peripheral nervous system (PNS), enhanced neuronal excitability in response to nerve injury may arise e.g. from dysregulated ion channel expression or the release of inflammatory mediators (Andersen et al., 2014).

3.2.2.1 Ion channel alteration

Nerve injury leads to increased expression of growth and transcription factors, which leads to nerve regeneration processes and to alterations of gene expression of receptors and ion channels (Baron et al., 2010). Especially voltage-gated sodium and calcium channels play an important role in pain transmission. Among several types of ion channels, the following channels have been shown to be crucial in stimulus detection and thus are potential druggable targets for analgesics.

The TRPV1 (transient receptor potential cation channel subfamily V member 1) ion channel is a known contributor to the perception of noxious heat. TRPV1, the receptor for capsaicin, has a thermal activation threshold of 43˚C, which meets the heat threshold of C and type II Aδ fibers (Caterina et al., 1997). Mice, lacking TRPV1 show severe impairment to detect noxious heat (Davis et al., 2000). Besides TRPV1,

other members of the transient receptor potential (TRP) family, like TRPV2, TRPV3 or TRPV4 are involved in heat sensation (Leffler et al., 2007;Lumpkin and Caterina, 2007).

TRPM8 (transient receptor potential cation channel subfamily M member 8) was identified as a cold-sensitive receptor, with a thermal activation threshold of 25˚C and menthol sensitivity. TRPM8 deficient mice show deficits in cold detection, but are not completely insensitive to cold stimuli. Further molecules, voltage-gated sodium and potassium channels are needed to evoke cold-induced action potentials (Basbaum et al., 2009).

Further evidence of the importance of voltage-gated sodium channels in pain states is provided by findings in patients with erythromelalgia or paroxysmal extreme pain disorder. These hereditary disorders that are characterized by severe pain are caused by gain-of-function mutations in the *SCN9A (*sodium voltage-gated channel alpha subunit 9) gene that encodes the Nav1.7 voltage-gated sodium channel (Hoeijmakers et al., 2015). In contrast, patients with loss of function mutations in this gene are unable to detect noxious stimuli (Dib-Hajj et al., 2017).

3.2.2.2 Immune system and pain

Inflammation is described as the response of an organism to tissue injury, including immune cell recruitment and release of inflammatory mediators. Besides, the immune system interacts with the sensory nervous system by altering the transduction of nociceptive information at nerve fiber, DRG, and synaptic terminal level (Calvo et al., 2012). Neuropathic pain is often associated with neuro-inflammation due to nerve lesions. After nerve damage Schwann cells and immune cells, like macrophages and mast cells are recruited to the injury site. The activation of the extracellular signal-related (ERK) mitogen-activated protein (MAP) kinase signaling pathway in Schwann cells leads to the release of inflammatory mediators, and as a result immune cells, including macrophages, T and B lymphocytes, neutrophils and dendritic cells infiltrate the damaged nerve (Napoli et al., 2012). Tracey and colleagues showed that depletion of macrophages in an animal model of neuropathic pain attenuates mechanical hypersensitivity (Liu et al., 2000). Lack of T lymphocytes in rats leads to reduced pain behavior after peripheral nerve injury (Moalem et al., 2004).

Inflammatory mediators can be subdivided into different classes such as cytokines, chemokines, proteolytic enzymes, lipid mediators, and neuropeptides (Ellis and Bennett, 2013).

Cytokines are small molecules, secreted by immune cells, fibroblasts, and Schwann cells and can be classified as pro- and anti-inflammatory. Pro-inflammatory cytokines (e.g. interleukin 1 [IL-1], IL-6, IL-12, and tumor necrosis factor-alpha [TNF]) act mostly algesic, whereas anti-inflammatory cytokines (e.g. IL-4, IL-10, IL-13) have an analgesic effect. However, depending on their concentration and location, cytokines can have pro- and anti-inflammatory properties (Turner et al., 2014). Data on disturbed pain behavior in animal models of cytokine deficiency underline the role of the immune system on pain (Cunha et al., 1999;Schoeniger-Skinner et al., 2007;Üçeyler et al., 2011;Sun et al., 2016).

Interactions between pro- and anti-inflammatory systems seem to play a major role in the pathophysiology of neuropathic pain (Calvo et al., 2012). One example is B7 homolog 1 (B7-H1), a major inhibitor of inflammatory responses (Freeman et al., 2000).

3.2.2.2.1 B7 homolog 1

B7-H1 (synonyms: PD-L1, CD274) is a type 1 transmembrane protein and a member of the B7/CD28 family (Dong et al., 1999;Ostrand-Rosenberg et al., 2014), which is expressed on non-lymphoid tissue, on activated macrophages and on dendritic cells. B7-H1 was identified as one of the two ligands for the programmed-death receptor-1 (PD-1; CD279) and its interaction with the B7-H1 receptor dampens immune responses, by inhibiting T cell receptor (TCR)/CD3 induced proliferation and cytokine production (Coyle and Gutierrez-Ramos, 2001). Furthermore, studies in B7-H1 deficient mice (B7-H1 ko) showed that B7-H1 reduces the secretion of pro-inflammatory mediators, IFN-γ and TNF-α (Latchman et al., 2001;Bodhankar et al., 2013). B7-H1 expression itself is induced by pro-inflammatory cytokines and growth factors like TNF and VEGF (vascular endothelial growth factor) (Boussiotis, 2016). Using the model of chronic constriction nerve injury, it has previously been shown that B7-H1 deficiency leads to an excessive pro-inflammatory response and prolonged and enhanced pain behavior after peripheral nerve lesion (Üçeyler et al., 2010), which makes B7-H1 an interesting candidate to study neuropathic pain pathomechanisms. The results of a recent study suggest that B7-H1 has anti-

nociceptive effects, by demonstating that B7-H1 suppressed formalin-induced inflammatory pain, neuropathic pain and bone cancer pain in rodents via the PD-1 receptor (Chen et al., 2017). Additionally, B7-H1 can be associated with several types of cancer and thus is a target in the development of new cancer therapies (Dong et al., 2002).

3.3 microRNA

MicroRNA (miRNA, miR) are non-coding single stranded RNA sequences (ncRNA) of 20-24 nucleotid length and are ubiquitously expressed across all tissue types. The first miRNA (lin-4) was discovered in *Caenorhabditis elegans* in 1993 (Lee et al., 1993). Later Pasquinelli and his group found analogous miRNA in several species, indicating a conserved principle of gene expression regulation (Pasquinelli et al., 2000). miRNA play a crucial role in diverse biological processes, ranging from embryonic development to disease pathologies including leukemia, cardiovascular diseases (Calin et al., 2004;Aboobaker et al., 2005;McManus and Freedman, 2015), and cancer (Tutar, 2014). Genes encoding miRNA are mostly intronic, thus their transcriptional regulation is similar to other genes, underlying the control by transcription factors and repressors. miRNA bind the respective mRNA sequences via a so called seed region, a sequence of 2-8 nucleotides, at the 5´ end of the mature miRNA (Lewis et al., 2005).

3.3.1 Biogenesis

miRNA biogenesis occurs via the canonical or non-canonical miRNA pathway. On the canonical pathway (Figure 2), the transcription of the miRNA gene by the RNA polymerase ll in the nucleus produces the primary miRNA (pri-miRNA), which has a large stem-loop structure. This pri-miRNA is recognized by Drosha-DGCR8 (DiGeorge syndrome critical region 8), which process the pri-miRNA to the precursor miRNA (pre-miRNA), which is exported to the cytoplasm by Exportin 5. In the cytoplasm, the pre-miRNA is further processed by Dicer–TRBP (TAR RNA-binding protein 2) and loaded into the Argonaute 2 (AGO2)‑containing RNA-induced silencing complex (RISC) (Ibrahim et al., 2012). Only the active strand is incorporated into the RISC, whereas the passive strand gets degraded. The active or mature strand of the miRNA is guided by the RISC to its target mRNA sequence. These sequences are often located in the 3’ untranslated regions (UTR), but can also be situated in the coding region or the 5’ UTR. Multiple copies in an mRNA sequence

lead to an enhanced effect on the target gene expression (Katz et al., 2016). During the non-canonical miRNA biogenesis the pre-miRNA are generated by a splicing machinery, avoiding the Drosha mediated processing in the nucleus (Li and Rana, 2014). There are two possible mechanisms to suppress downstream target gene expression: imperfect base pairing leads to translational repression, while an extensive base pairing induces mRNA cleavage.

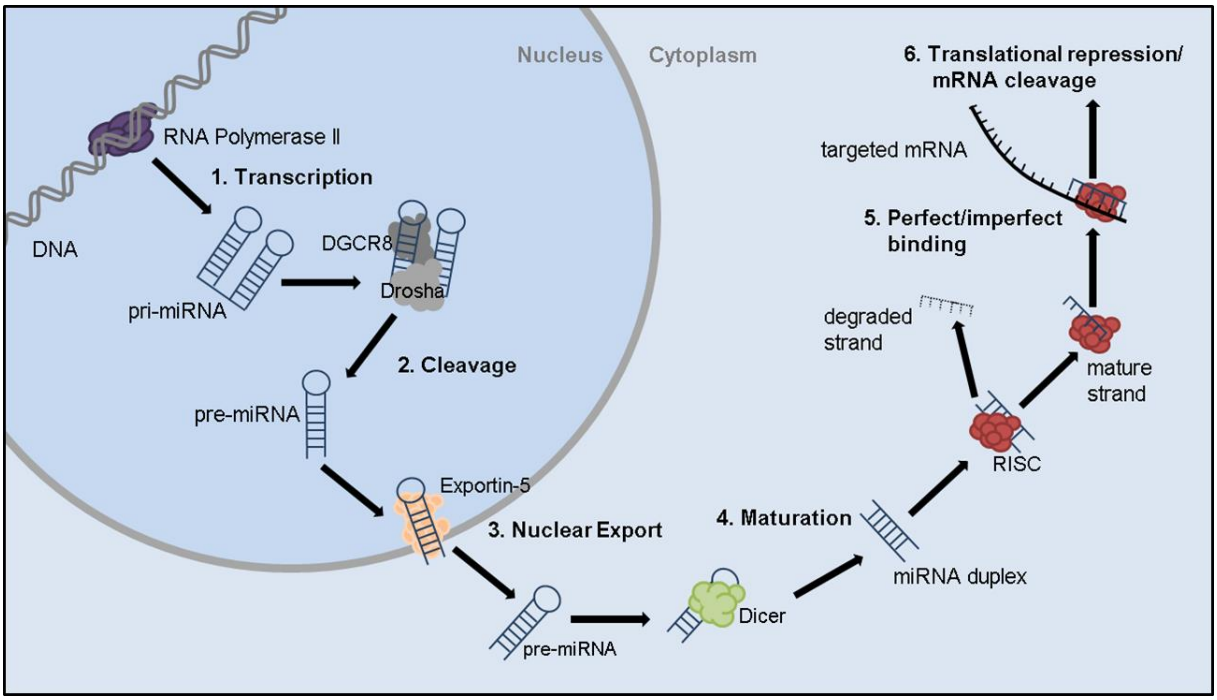

Figure 2: Schematic illustration of canonical microRNA (miRNA) biogenesis and function. (1.) miRNA gene is transcribed in the nucleus. (2.) The primary miRNA (pri-miRNA) is cleaved by Drosha and DiGeorge syndrome critical region gene 8 (DGCR8) to the precursor miRNA (pre-miRNA), which is exported to the cytoplasm by Exportin-5 (3.), where further maturation is performed by Dicer (4.). The mature miRNA strand is loaded into the RNA-induced silencing complex (RISC) and guided to the 3' untranslated region (UTR) of the messenger RNA (5.). Perfect or imperfect complementary binding of the mRNA leads to mRNA cleavage or translational repression (6.).

3.3.2 Target prediction

There are several online and offline databases for bioinformatical, sequence-based miRNA target prediction, like TargetScan, DIANA-microT, miTarget, PITA, MIRZA, and many more. These databases use different algorithms to computationally predict miRNA-mRNA interaction. For example TargetScan is using the 7mer-m8 region in the seed sequence for target prediction, while PITA explores the complementarity applying 6mer seed type (Fan and Kurgan, 2015). Some databases, like TargetScan and miTarget, use the information about AU content around the target, while others neglect this information. The AU content in the mRNA 3' UTR is important for the

interaction with miRNA (Hoffman et al., 2013). Some target prediction tools consider binding to the target gene with multiple predicted sites, which enhances the mRNA regulation (Saito and Saetrom, 2012). These different approaches hamper output comparisons of diverse databases. However, considering specificity and precision of the predictive performance at gene or duplex level may help users select the appropriate prediction method for their experiments (Fan and Kurgan, 2015). Another database is miRTarBase, which is based on surveying published literature about experimentally validated miRNA–target interactions (MTI). There are other MTI databases with smaller and less abundant collections, like TarBase and miRecords (Hsu et al., 2011). One major problem is that the application of distinct algorithms results in various predicted mRNA targets. One approach to solve this problem is, using several prediction algorithms in parallel and choosing only consistently predicted targets (Bali and Kuner, 2014).

3.3.3 Tools for miRNA interference

There are several tools available to influence miRNA expression in vivo by either mimicking or antagonizing miRNA. By using miRNA mimics, which are double stranded RNA molecules, it is possible to upregulate endogenous miRNA. Inhibition of endogenous miRNA can be achieved by using anti-miRNA oligonucleotides. These miRNA inhibitors are chemically modified, like changes of individual nucleotides or backbone alterations, to facilitate cellular uptake and to avoid degradation. One oligonucleotide variation is the locked nucleic acid (LNA), a bicyclic nucleic acid that binds the 2’ oxygen to the 4’ carbon via a methylene bridge, locking the structure into a 3’ endo confirmation. LNA offers the biggest success in improving the binding affinity among the oligonucleotide modifications and has a good nuclease resistance (Li and Rana, 2014). Since getting miRNA inhibitors or mimics into the target tissue is challenging, chemical reagents, like transfection agents, are additionally used to improve the delivery. Furthermore, the use of adenovirus, lentivirus or herpes simplex virus, encoding miRNA inhibitors or pre-miRNA, is recommended for miRNA in vivo modulation (Bali and Kuner, 2014).

3.4 Clinical development of miRNA therapeutics

Since chemically modified oligonucleotides have been efficient in blocking miRNA function in vitro and in preclinical animal models, efforts have been made to advance clinical development of therapeutic oligonucleotides. First evidence for a role of

miRNA in human diseases came from cancer research after having discovered that miRNAs are frequently located in fragile regions of cancer genome. In several studies the miR-34 family was identified as a crucial regulator of cell growth and as being downregulated in diverse cancer cells (Calin et al., 2004;Iorio and Croce, 2012). Several studies reported that delivery of a miR-34 mimic decreased tumor growth and led to lower levels of miR-34 regulated proteins like MET or B-cell lymphoma 2 in mouse models of liver, prostate, and lung cancer (Wiggins et al., 2010;Liu et al., 2011a). MRX34, a miR-34 mimic encapsulated in a liposome vesicle, was developed by Mirna Therapeutics and is the first miRNA mimic that has entered a phase one clinical trial in primary hepatic cancer patients or solid cancers with liver involvement (Bouchie, 2013). The MRX34 replacement therapy restores the lost suppressor function of miR-34 by delivering a miR-34 mimic. However, due to immune-related adverse events the study was terminated and preclinical trials need to be redesigned considering immune toxicity (Rupaimoole and Slack, 2017).

Other miRNA, like miR-21 and let-7 (lethal 7) have also been associated with cancer and different pharmaceutic companies are developing potentially therapeutic miRNA inhibitors for clinical use. In 2005, miR-122 was identified as a liver-specific miRNA, that modulates hepatitis C virus (HCV) replication (Jopling et al., 2005). Santaris Pharma developed the first miRNA targeting drug, a miR-122 inhibitor (miravirsen) that entered clinical trials. Miravirsen decreased HCV RNA serum levels after five weekly subcutaneous injections in patients with chronic HCV infection in a phase II study and may be launched as the first anti-miRNA drug in near future (Li and Rana, 2014).

These data suggest that miRNA may become attractive therapeutic targets and promise the availability of miRNA-associated drugs on the market in the next years for treatment of diverse diseases. However, the precise mode of action is still unknown and in-depth biochemical analysis is needed, to gain further knowledge enabling higher stability, tissue specificity, and less off-target effects (van Rooij et al., 2012).

3.5 miRNA and pain

Due to several mediators and pathways potentially contributing to neuropathic pain, targeting one single molecule is not sufficient for analgesic treatment (Niederberger et al., 2011). Since the miRNA-mRNA functional pairing does not need a fully

complementary sequence, miRNA are able to bind to several mRNA and thus can simultaneously influence multiple mediators in different pain pathways (Lewis et al., 2005;Bali and Kuner, 2014).

The first indication of miRNA being involved in pain was provided by a specific conditional Dicer knockout mouse (Dicer deletion in damage-sensing neurons that express Nav1.8) that showed less pain behavior upon application of inflammatory mediators compared to homozygous floxed *dicer* littermates (Zhao et al., 2010). Recent research in animal models identified several miRNA as being crucially involved in pain pathways (Bali and Kuner, 2014). Examples are miR-96, miR-182, and miR-183, a sensory organ-specific cluster of microRNA, which were downregulated after SNL in DRG of adult rats (Aldrich et al., 2009). Another study indicated that lentivirion-mediated miR-183 expression attenuates SNL-induced mechanical allodynia (Lin et al., 2014). Kusuda et al. analyzed the expression of three miRNA (miR-1, miR-16, miR-206) under inflammatory and neuropathic pain conditions. They found a decrease of the investigated miRNA in DRG in an inflammatory pain model, while all three miRNA were upregulated after axotomy. Even across different neuropathic pain models, miRNA were differentially expressed, suggesting that miRNA expression profiling results should be evaluated carefully considering the method and the time point tested (Kusuda et al., 2011).

One further miRNA, which could be linked to pain in animal models, is miR-21. miR-21 was upregulated in the sciatic nerve, in the spinal cord, and in DRG in diverse models of neuropathic pain in mice and rats (Strickland et al., 2011;Wu et al., 2011;Genda et al., 2013;Hori et al., 2016). Pain behavior could be relieved by intrathecal administration of a miR-21 inhibitor in rats (Sakai and Suzuki, 2013).

Several studies also reported that miR-21 controls the balance between pro- and anti-inflammatory responses in leukocytes and non-hematopoietic cells (Sheedy, 2015). Some miRNA have been shown to regulate neuronal and immune gene expression simultaneously, which makes these so called ‘NeuimmiRs’ promising targets for master switches that might be of particular importance in neuropathic pain pathophysiology (Soreq and Wolf, 2011;Wanet et al., 2012). Besides miR-21 one further NeuimmiR candidate is miR-132-3p. In a recent study white blood cells and sural nerve biopsies of patients with peripheral neuropathies and in parallel spinal cord of rats treated with SNI was investigated and an increase in neural miR-132-3p

expression was found in rats and in patients suffering from neuropathic pain compared to those without pain. In vivo modulation of miR-132-3p using an inhibitor or mimic attenuated or induced pain behavior in rats respectively (Leinders et al., 2016b).

First evidence for dysregulation of miRNA in blood samples of patients with pain syndromes was reported by Orlova et al. in 2011. By using a TaqMan array, the group found 18 differentially expressed miRNA in blood samples of patients with complex regional pain syndrome (CRPS) (Orlova et al., 2011). In another study the same group investigated miRNA in serum-derived exosomes of CRPS patients and demonstrated that the miRNA signature differed from that obtained in whole blood. The expression of only one miRNA (miR-25-3p) showed the same trend in whole exosomes and blood in CRPS patients (McDonald et al., 2014). Others reported that eight miRNA are differentially expressed in peripheral blood mononuclear cells and in serum samples of patients with fibromyalgia syndrome (Bjersing et al., 2015;Cerda-Olmedo et al., 2015). However, the altered miRNA expression differed between both reports, indicating the importance of the miRNA source. Recent studies in sera of patients with migraine attacks demonstrated that miR-34a-5p and miR-382-5p were upregulated (Andersen et al., 2016), whereas miR-124a and miR-155 were increased in T cells of patients with neuropathic pain compared to healthy controls (Heyn et al., 2016). Also, miR-let-7d was found associated with pain and aberrantly expressed in skin samples of patients with fibromyalgia syndrome (Leinders et al., 2016a).

3.6 Aim of the study

miRNA are increasingly recognized as regulators of immune and neuronal gene expression and are potential master switches in neuropathic pain pathophysiology. miR-21 is a promising candidate that may link the immune system and pain mediators. In previous studies B7-H1 has been identified as a major inhibitor of inflammatory response. The aim of this study was to investigate the potential link between B7-H1 and miR-21 in inflammation and neuropathic pain by addressing the following questions:

- Does the lack of B7-H1 determine the pain phenotype after SNI and does miR-21 inhibition influence the pain phenotype?

- Does neuropathic pain influence affective and cognitive behavior in B7-H1 ko and WT mice?

- Are there changes in miR-21 expression in neuronal tissue after SNI?

- Is there an enhanced inflammatory response in B7-H1 ko mice after SNI?

4 Material and Methods

4.1 Equipment, buffers and solutions, antibodies, and primer sequences

Technical equipment (Appendix 8.1), reagents (Appendix 8.2), buffers and solutions (Appendix 8.3) as well as primer sequences for genotyping and quantitative real-time-PCR (qRT-PCR) (Appendix 8.5) and antibodies for immunohistochemistry (Appendix 8.6) are detailed in the appendices.

4.2 Animals and genotyping

B7-H1 ko mice were generated by L. Chen, Baltimore, USA (Dong et al., 2004) and inbred wildtype littermates (WT) of C57Bl/6J background served as controls. Genotypes were identified after purification of genomic DNA from ear biopsies using the DNeasy blood&tissue kit (Qiagen, Hilden, Germany) according to the manufacturer's instructions. The Kapa2G fast PCR Kit (Kapa Biosystems, Wilmington, USA) was used to determine the genotypes by conventional PCR (respective primer sequences listed in Appendix 8.4). We investigated mice of three age-groups: young (8 weeks), middle-aged (6 months), and old (12 months) mice. *B7-H1* gene expression was determined in young and old WT mice, to exclude changes in B7-H1 expression due to ageing (Figure 3).

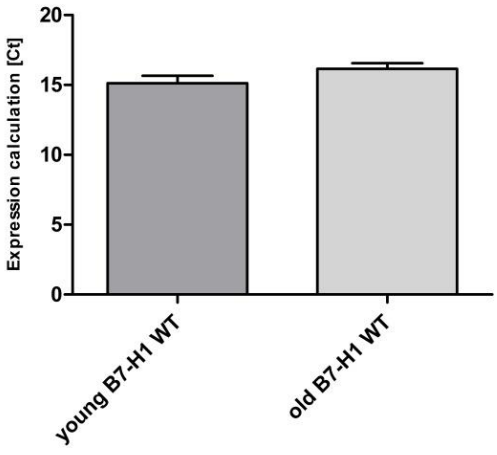

Figure 3: Expression calculation of B7-H1 revealed by quantitative real-time-PCR. *B7-H1* expression did not differ between young (8 weeks) and old (12 months) WT mice.

C57Bl/J and C57BL/N mice for analyses were purchased from Charles River (Charles River Laboratories, Wilmington, USA).

All experiments were approved by the Bavarian State authorities (Regierung von Unterfranken, #3/12). Mice were housed in the animal facilities of the University of Würzburg (Department of Neurology; Center for Experimental Molecular Medicine), in a 12 h/12 h day (<300 lux)/night rhythm with food and water access *ad libitum*. Animal use and care were in accordance with the institutional guidelines.

4.3 Behavioral testing

All behavioral tests were performed by an experienced investigator (FK) blinded to the genotype. Mice of three age-groups (young [8 weeks], middle-aged [6 months], and old [12 months] mice) were investigated for mechanical and thermal sensitivity. For affective and cognitive behavior we concentrated on young and old mice.

4.3.1 Mechanical and thermal sensitivity

All mice were tested three times before surgery to obtain baseline values and to allow the animals to get used to the testing apparatus. Behavioral tests were performed at selected time points 3, 7, and 14 days after SNI (n= 6 mice/genotype and age-group). The von-Frey test based on the up-and-down-method was used to investigate the paw withdrawal thresholds upon mechanical stimulation. Animals were placed in individual acrylic glass boxes on a wire mesh. After 45 min adaption, the lateral plantar surface of the hind paws (i.e. sural nerve innervation territory) was touched with a von-Frey filament starting at 0.69 g. If the mouse withdrew its hind paw, the next finer von-Frey filament was used. If the mouse did not show any reaction, the next thicker von-Frey filament was applied. Each hind paw was tested six times. The 50 % withdrawal threshold (i.e. force of the von-Frey hair to which an animal reacts in 50 % of the administrations) was calculated.

The Hargreaves method using a standard Ugo Basile Algometer (Comerio, Italy) was applied to determine the sensitivity to thermal heat stimuli (Hargreaves et al., 1988). Mice were individually placed on a glass surface in acrylic glass boxes. After 45 min adaption, a radiant heat stimulus (25 IR) was applied to the lateral plantar surface of the hind paw and the withdrawal latency was automatically recorded. To prevent tissue damage by heat, we used a stimulus cut-off time of 16 s. Each hind paw was tested three times.

The cold plantar test was used to determine paw withdrawal latencies to cold stimuli (Brenner et al., 2012). Mice were placed in individual acrylic glass boxeson a glass

surface (1/4 ´´) and a dry ice stick was applied against the glass at the lateral plantar side of the hind paw (i.e. sural nerve innervation territory). Time until paw withdrawal was recorded with a limit for stimulus application of 20 s to avoid tissue damage.

4.3.2 Tests for affective and cognitive behavior

Mice were housed in a reversed light-dark cycle (light cycle: 7 p.m.-7 a.m.; dark cycle: 7 a.m.-7 p.m.) and were tested under infra-red light during the dark cycle, in their active phase. To avoid interference with other mice and the investigator, all behavioral tests were performed in a black box. Tests were carried out following the algorithm shown in (Figure 4). All tests were video recorded for further analysis (see below).

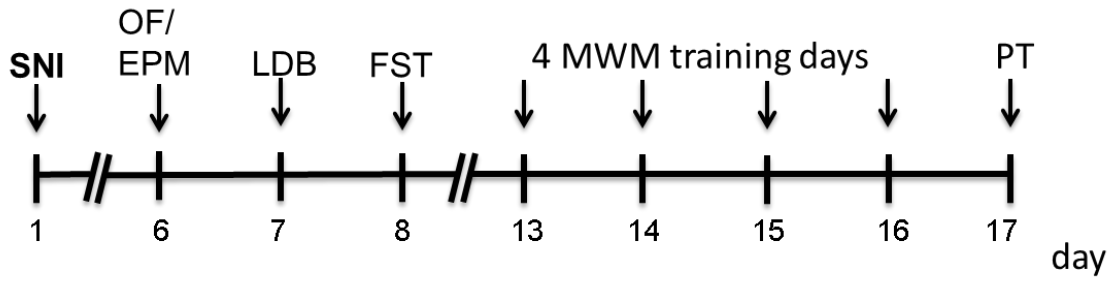

Figure 4: Experimental design of tests for affective and cognitive behavior. Young (8 weeks) and old (12 months) mice were tested after spared nerve injury (SNI) in the following sequence: elevated plus maze (EPM), open field (OF), light-dark box (LDB), forced-swim test (FST), Morris water maze test (MWM) and Morris water maze probe trail (PT).

4.3.2.1 Anxiety- and depression-like behavior

For the assessment of the intra-individual variation in affective behavior, we performed three different tests for anxiety: light-dark box (LDB) (Crawley and Goodwin, 1980), elevated plus maze (EPM) (Pellow et al., 1985), and open field (OF) (Prut and Belzung, 2003). EPM and OF were also used to investigate exploratory behavior of the mice. Mice were tested individually for 5 min in each apparatus and only once to avoid the influence of learning on behavior.

The LDB consisted of an illuminated (40 cm x 20.5 cm) and a dark compartment (40 cm x 19.5 cm). As a starting point, each mouse was placed in the lit box. Mice could freely explore the apparatus and choose between the two inter-connected compartments. The percentage of time spent in the dark box was recorded.

The EPM apparatus consisted of two opposite open arms (66.5 cm) and two closed arms (65.5 cm), which are separated by a junction area. Mice were individually

placed in the middle of the apparatus, facing an open arm. The total time spent in closed arms, the entries into open arms, and the total distance travelled were recorded.

The OF (40 cm x 40 cm) consisted of two areas: the center zone (20 cm x 20 cm) and the surrounding area. To start the test, mice were placed in the middle of the center zone. Time spent in the center zone, the total distance travelled, and the average speed were determined.

To test for depression-like behavior we performed the forced-swim test (Porsolt et al., 1977). Mice were individually placed in a glass cylinder, filled with water (diameter of cylinder: 11.5 cm; water height: 12.5 cm; water temperature: 20 °C ±2 °C). Within a six min testing phase the time spent immobile was measured during an observation period of five min (2.-6. min).

4.3.2.2 Cognitive behavior

The Morris water maze test (MWM) (Morris, 1984) was used to investigate learning behavior and memory. Tests were performed in a cylindric plastic pool (diameter: 118. 5 cm), filled with water (temperature: 20 °C ±2 °C) just covering the platform (diameter: 8 cm). Opaque water was used to avoid visibility of the platform. The pool was divided into four quadrants and the platform was placed in the south-east quadrant (= target quadrant). During the MWM training days, mice had four daily trails with different starting points (located in the middle of each quadrant) on four consecutive days. The time mice needed to reach the platform was measured and the daily average time for every group was calculated. Mice that did not find the platform within 60 s were placed on the platform for 15 s for orientation in the pool and to remember the location of the platform. On the fifth day we performed the probe trail (PT) for memory performance, during which the platform was removed. We chose a new starting point on the opposite side of the target quadrant for the PT. Time mice spent in the target quadrant, the total distance they swam, and the average speed was measured during a 30 s observation period.

4.4 Spared nerve injury (SNI)

Naïve mice were anesthetized with isoflurane (2 % induction, 1.5 % maintenance) in a 50 % O_2/room air mixture. SNI or a sham surgery was performed as described (Decosterd and Woolf, 2000). Skin on the lateral surface of the right thigh was incised

and the sciatic nerve and its three branches were exposed by a blunt dissection through the biceps femoris muscle. The common peroneal and the tibial nerves were ligated (using 7.0 silk) distal to the trifurcation of the sciatic nerve and dissected distal to the ligation (Figure 5), removing a 2–4 mm piece of each nerve stump. Great care was taken to keep the sural nerve untouched. Incisions were closed with muscle and skin sutures in two layers. In sham surgery, the sciatic nerve branches were exposed, but not injured. After surgery, mice were kept at 37 °C until they regained consciousness. Behavioral experiments were conducted 3 to 21 days after surgery.

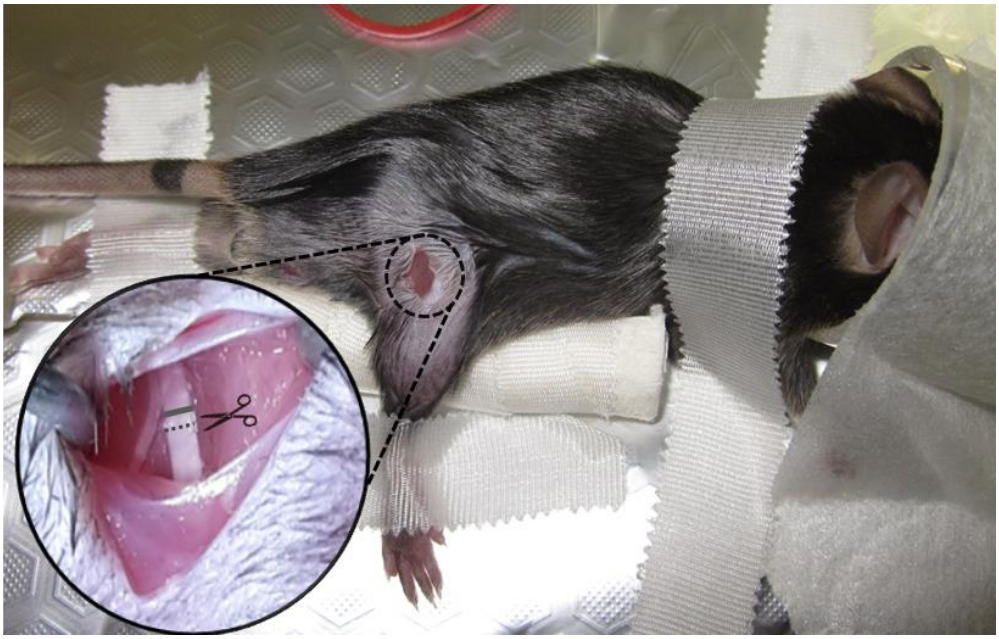

Figure 5: Spared nerve injury (SNI) surgical procedure. Photomicrograph of an anesthetized mouse with immobilized hind paw. Magnification shows the exposed sciatic nerve at trifurcation. The tibial and the common peroneal nerve are ligated. The dotted line marks the location, where the nerves are transected. The sural nerve (left) is spared.

4.5 Perineurial injection of miR-21 inhibitor

A LNA based in vivo inhibitor for miR-21-5p (Exiqon, Vedbaek, Denmark) and a mismatch control (scrambled oligonucleotide, Scr) were injected transdermally and perineurially using a microsyringe fitted with a 27-gauge needle. The femur head was used as a landmark to find the sciatic nerve (Ma and Quirion, 2006). In pilot studies perineurial injections of trypan blue confirmed the correct application of the dye next to the trifurcation of the sciatic nerve using this injection technique. Prior to the injection, the miRNA inhibitor and the mismatch control were mixed (1:5 w/v) with the in vivo transfection agent i-Fect™ (Neuromics, Edina, USA) to a final concentration of 0.1 pmol/µl. Mice were anesthetized with 1.5 % isoflurane in a 50 % O_2/room air

mixture and received perineurial injections of 50 µl every 24 h on 5 consecutive days, starting on day 3 after SNI (Figure 6). Mechanical and heat sensitivity were tested 5 h after each injection. On day 11 after surgery we assessed mechanical and thermal sensitivity without perineurial injection of miR-21-5p inhibitor.

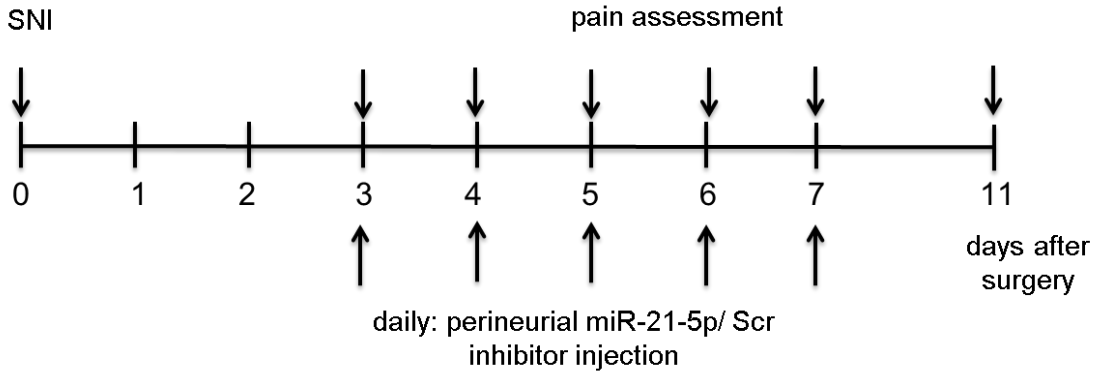

Figure 6: Experimental design of miR-21-5p inhibition. Old (12 months) mice underwent spared nerve injury (SNI) and received daily perineurial injections of the miR-21-5p inhibitor or the mismatch control (Scr) 3-7 days after surgery. Mechanical and thermal sensitivity (pain assessment) was tested 5 h after injection. On day 11 after surgery mice were tested without injection of miR-21-5p inhibitor.

4.6 Tissue collection

At the end of the experiments mice were sacrificed in deep isoflurane anesthesia and the ipsilateral nerve stump (common peroneal and tibial nerve) of the sciatic nerve (proximal to the nerve injury), the sural nerve, the DRG, and the lumbar spinal cord were dissected for qRT-PCR using a dissection microscope (Zeiss, Oberkochen, Germany) at the following time points: baseline, 7, 15 days after SNI (n= 6 mice/ age-group). Tissue from naïve mice served as controls. Tissue was shock frozen in liquid nitrogen and was stored at -80 °C until further processing. For immunohistochemistry the ipsilateral nerve stump (common peroneal and tibial nerve) of the sciatic nerve and the sural nerve (n= 5 per group) were dissected 7 days after SNI. Tissue was embedded in Tissue Tek, OCT medium (optimal cutting temperature; Sakura, Staufen, Germany), frozen in liquid nitrogen cooled 2-methylbutane, and stored at -80 °C until further processing. Blood was withdrawn in deep isoflurane anaesthesia via cardiac puncture after thoracotomy.

4.7 qRT-PCR studies

Total RNA from dissected tissue was isolated using the miRNeasy Micro Kit (Qiagen, Hilden, Germany); for total RNA extraction from white blood cells (WBC) the Leukocyte RNA purification kit (Norgen biotek corp., Thorold, Canada) was used

following the manufacturers` recommendations. RNA concentration was quantified spectrophotometrically with the NanoPhotometer Pearl® (Implen, Munich, Germany). For gene expression analysis of *B7-H1* levels (Cd274, Assay ID: Mm03048248_m1) TaqMan qRT-PCR (Applied Biosystems, Darmstadt, Germany) was used. 150 ng total RNA was reverse transcribed using TaqMan Reverse Transcription Reagents, following manufacturer's protocol. PCR reagents were used from Life Technologies (Carlsbad, CA). For each sample 5 µl cDNA was applied. 18sRNA (Assay ID: Hs99999901_s1) was used as an endogenous control.

For miRNA-specific synthesis of first strand cDNA, 5 ng of total RNA was transcribed using the Universal cDNA Synthesis kit II (Exiqon, Vedbaek, Denmark) following the manufacturer's protocol. For each reaction 4 µl of diluted (1:80) cDNA was amplified applying the corresponding miRNA and reference primer sets, using the miCURY LNA™ Universal microRNA PCR (Exiqon, Vedbaek, Denmark) following the manufacturer's protocol. The expression levels of miR-21-5p were normalized to the expression of the endogenous control Sno202 (respective primer sequences listed in appendix 8.5). Sno202 from Exiqon was chosen as an endogenous control for individual target normalization since it showed the most stable qRT-PCR results among several different candidates (Exiqon: RNU5G, Snord110, U6, 5S, U1A1, Snord65, Snord68; TaqMan: Sno202, Sno234) tested before and after SNI (Figure 7). For testing Sno202 and Sno234 from TaqMan TaqMan®Micro RNA RT Kit and TaqMan®Universal PCR Master Mix was used following the provided protocols.

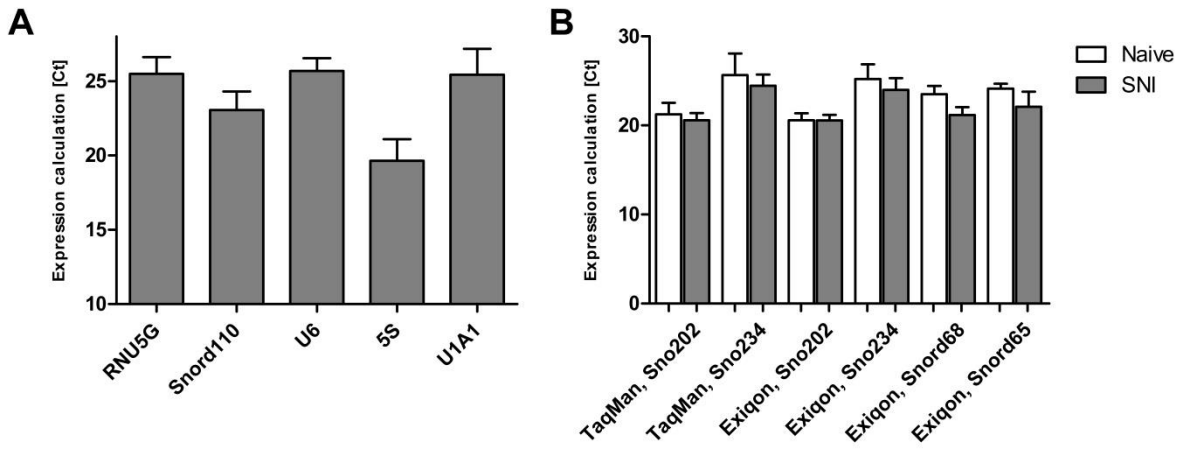

Figure 7: Expression of different endogenous controls in mouse nervous tissue. (A) RNU5G, Snord110, U6, 5S, and U1A1 from Exiqon were not expressed in a stable manner. (B) Sno202 from Exiqon showed the most stable expression comparing naïve tissue to tissue dissected after spared nerve injury (SNI). n≥6 per target.

miR-21 was amplified in triplicate and threshold cycle (Ct) values were obtained. Fold changes in miRNA expression among groups were calculated using the delta-delta Ct method.

4.8 Immunohistochemistry

Ten-µm cryosections of the common peroneal/tibial nerve and the sural nerve were prepared using a cryostat (Leica, Blenheim, Germany). Immunohistochemical staining with antibodies against CD11b (Serotec, Puchheim, Germany) for the detection of monocytes/macrophages (further referred to in the text as "macrophages") and CD3 (Serotec, Puchheim, Germany) for the detection of T cells were performed. Briefly, after acetone fixation and blocking with 10 % BSA in 0.1 M PBS (30 min at RT) respective primary antibodies were incubated over night at 4 °C in 1 % BSA/Tris. Sections were incubated with the secondary antibodies (anti-rat IgG), followed by Avidin/Biotin blocking (Vector Laboratories, Burlingame, USA) before visualization by 0.02 % diaminobenzidine (DAB). Haemalaun was used as a counter staining of the nuclei. On negative control sections the primary antibody was omitted. All samples were embedded with Vitro-Clud® (Langenbrinck GmbH, Emmendingen, Germany). Detailed information about the antibodies used in this study can be found in Appendix 8.6.

Images were acquired using an Axiophot 2 microscope (Zeiss, Oberkochen, Germany) equipped with a CCD camera (Visitron Systems, Tuchheim, Germany). Immuno-positive profiles were quantified manually in at least three nerve sections for each mouse and were related to the area of the nerve sections. The investigator was blinded to the genotype and treatment. Data were analyzed using SPOT software (software version 5.2, Spot Software BV, Amsterdam, Netherlands) and ImageJ free software version 1.51f (National Institute of Health, Staten Island, USA).

4.9 Video processing and statistical analysis

Recorded videos from the affective and cognitive behavior tests were analyzed using the ANY-maze video tracking software (system version: 4.99m, Stoelting, USA). For statistical analysis SPSS IBM software Version 23 was employed (Ehningen, Germany). The non-parametric Mann-Whitney U test was applied, since data were not normally distributed in the Kolmogorov-Smirnov test. Data are illustrated as box plots, bar graphs or line charts as appropriate (SPSS IBM software version 23 and GraphPad Prism, software version 5.03, San Diego, CA, USA). Data were stratified

for age (young: 8 weeks, middle-aged: 6 months, old: 12 months) and treatment groups (naïve, sham, SNI). P values <0.05 were considered statistically significant. Data of the qRT-PCR are illustrated as box plots, representing the median value and the upper and lower 25 % and 75 % quartile. All other data were expressed in bar graphs or line charts as mean with standard error of the mean.

5 Results

5.1 Mechanical and heat hypersensitivity in B7-H1 ko and WT mice after SNI

Naïve young ($p<0.01$) and middle-aged ($p<0.05$) B7-H1 ko mice showed mechanical hypersensitivity compared to WT mice, whereas mechanical thresholds did not differ between old B7-H1 ko and WT mice (Figure 8 A). Young, middle-aged, and old B7-H1 ko and WT mice developed mechanical hypersensitivity after surgery, already detectable on day three after surgery ($p<0.01$ each, Fig. 8 B-D). No differences between genotypes were detected after SNI.

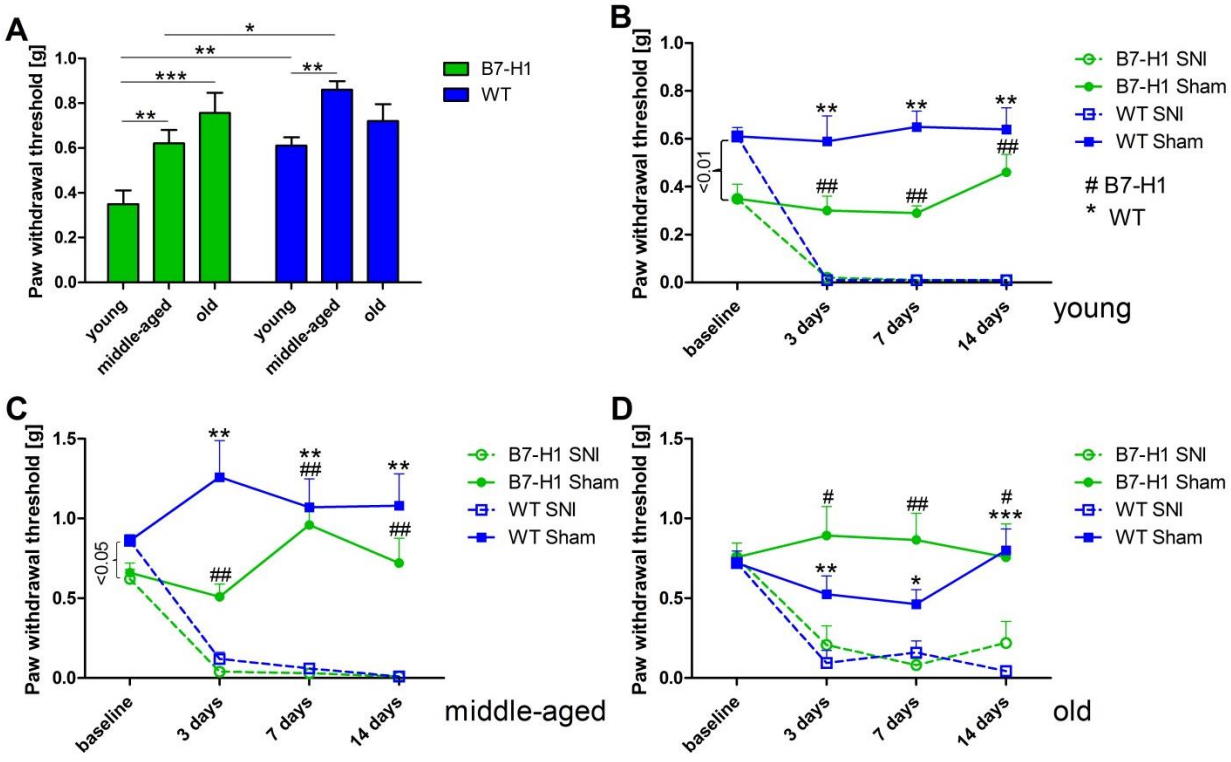

Figure 8: Paw withdrawal thresholds to mechanical stimulation. Results of the von-Frey test in young (8 weeks), middle-aged (6 months), and old (12 months) B7-H1 ko and wildtype littermate (WT) mice at baseline and 3, 7, and 14 days after spared nerve injury (SNI) or sham surgery are shown in bar graph and line charts. (A) Young ($p<0.01$) and middle-aged ($p<0.05$) B7-H1 ko mice in the naïve state displayed mechanical hypersensitivity compared to WT mice. At baseline mechanical thresholds were lower in young (B) and middle-aged (C) B7-H1 ko mice compared to WT mice ($p< 0.01$, $p< 0.05$). Mechanical perception did not differ in old (D) B7-H1 ko and WT mice in at baseline. Young, middle-aged and old B7-H1 ko and WT mice developed mechanical hypersensitivity 3 days (young/middle-aged: $p<0.01$; old: B7-H1 $p< 0.05$, WT $p<0.01$), 7 days (young/middle-aged: $p< 0.01$; old: B7-H1 $p<0.001$, WT $p<0.05$), and 14 days (young/middle-aged: $p< 0.01$; old: B7-H1 $p<0.05$, WT $p<0.001$) after SNI without differences between both genotypes. Mechanical withdrawal thresholds of sham operated B7-H1 ko and WT mice did not differ from baseline values 3, 7, and 14 days after surgery.

B7-H1 ko: young (8 weeks; SNI: 4 male, 2 female; sham: 2 male, 2 female), middle-aged (6 months; SNI: 3 male, 3 female; sham: 3 male, 3 female), old (12 months, SNI: 3 male, 5 female; sham: 3 male, 3 female).
WT: young (8 weeks; SNI: 3 male, 3 female; sham: 3 male, 3 female), middle-aged (6 months; SNI: 3 male, 3 female; sham: 3 male, 3 female), old (12 months, SNI: 3 male, 5 female; sham: 3 male, 4 female).
*, # p<0.05; **, ## p<0.01; ***, ### p<0.001.

At baseline, heat withdrawal latencies did not show differences between B7-H1 ko and WT mice in any age-group. From day three after SNI, both genotypes developed heat hypersensitivity without intergroup differences (p<0.01, Figure 9).

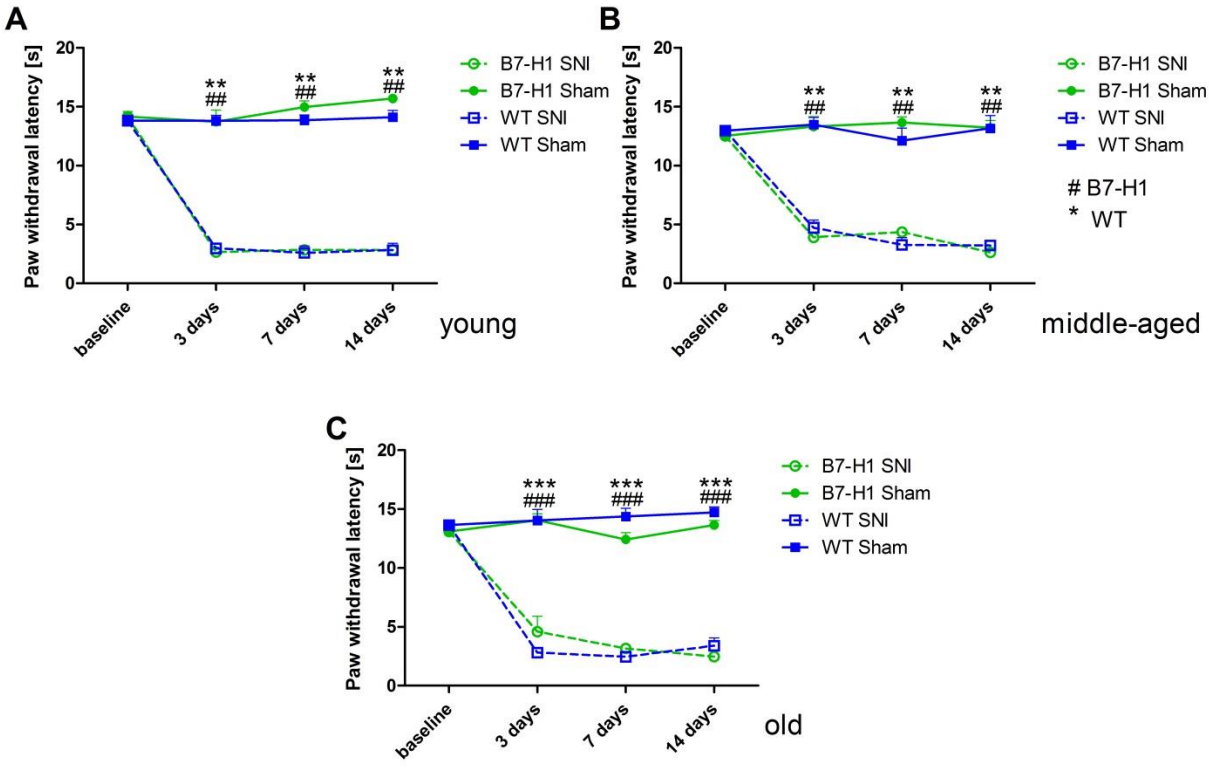

Figure 9: Paw withdrawal latencies to heat stimulation. Results of the Hargreaves test in young (8 weeks), middle-aged (6 months), and old (12 months) B7-H1 ko and wildtype littermate (WT) mice at baseline and 3, 7, and 14 days after spared nerve injury (SNI) or sham surgery are shown in line charts. No difference for paw withdrawal latencies to heat stimulation was detected in young (A), middle-aged (B), and old (C) B7-H1 ko and WT mice. Young, middle-aged and old B7-H1 ko and WT mice developed hypersensitivity to heat stimuli 3, 7, and 14 days after SNI without intergroup differences (young, middle-aged: p<0.01, old: p<0.001). Sham operated B7-H1 ko and WT mice did not differ 3, 7, and 14 days after surgery.
B7-H1 ko: young (8 weeks; SNI: 4 male, 2 female; sham: 2 male, 2 female), middle-aged (6 months; SNI: 3 male, 3 female; sham: 3 male, 3 female), old (12 months, SNI: 3 male, 5 female; sham: 3 male, 3 female).
WT: young (8 weeks; SNI: 3 male, 3 female; sham: 3 male, 3 female), middle-aged (6 months; SNI: 3 male, 3 female; sham: 3 male, 3 female), old (12 months, SNI: 3 male, 5 female; sham: 3 male, 4 female).
, ## p<0.01; *, ### p<0.001.

Cold withdrawal latencies were normal at baseline and did not change after SNI in both genotypes and age-groups (Figure 10).

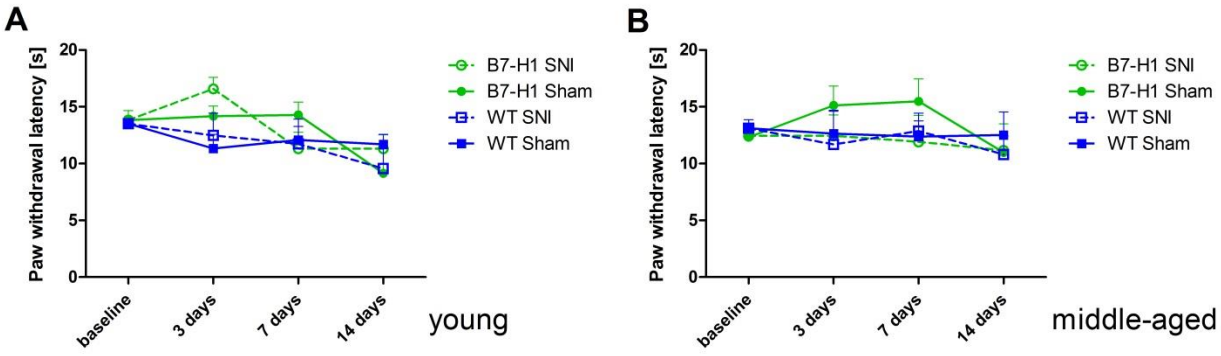

Figure 10: Paw withdrawal latencies to cold stimulation. Results of the cold plantar test in young (8 weeks) and middle-aged (6 months) B7-H1 ko and wildtype (WT) mice at baseline and 3, 7, and 14 days after spared nerve injury (SNI) are shown in linecharts. Young (A) and middle-aged (B) B7-H1 ko did differ in cold sensitivity at baseline and 3, 7, and 14 days after SNI compared to WT mice.
B7-H1 ko: young (8 weeks; SNI: 4 male, 2 female; sham: 2 male, 2 female), middle-aged (6 months; SNI: 3 male, 3 female; sham: 3 male, 3 female).
WT: young (8 weeks; SNI: 3 male, 3 female; sham: 3 male, 3 female), middle-aged (6 months; SNI: 3 male, 3 female; sham: 3 male, 3 female).

5.2 No influence of SNI on anxiety-like behavior

In the LDB test, the time mice stayed in the dark compartment of the LDB did not differ between young B7-H1 ko and WT mice in the naïve state or after SNI (Figure 11 A). Also in the EPM, no differences were detected in the time mice spent in the closed arms (Figure 11 B), and in the number of entries into open arms between both genotypes and surgeries (Figure 11 C). Exploratory behavior was assessed by measuring the total distance travelled in the EPM and decreased only in WT mice after SNI ($p<0.05$, Figure 11 D) without intergroup difference.

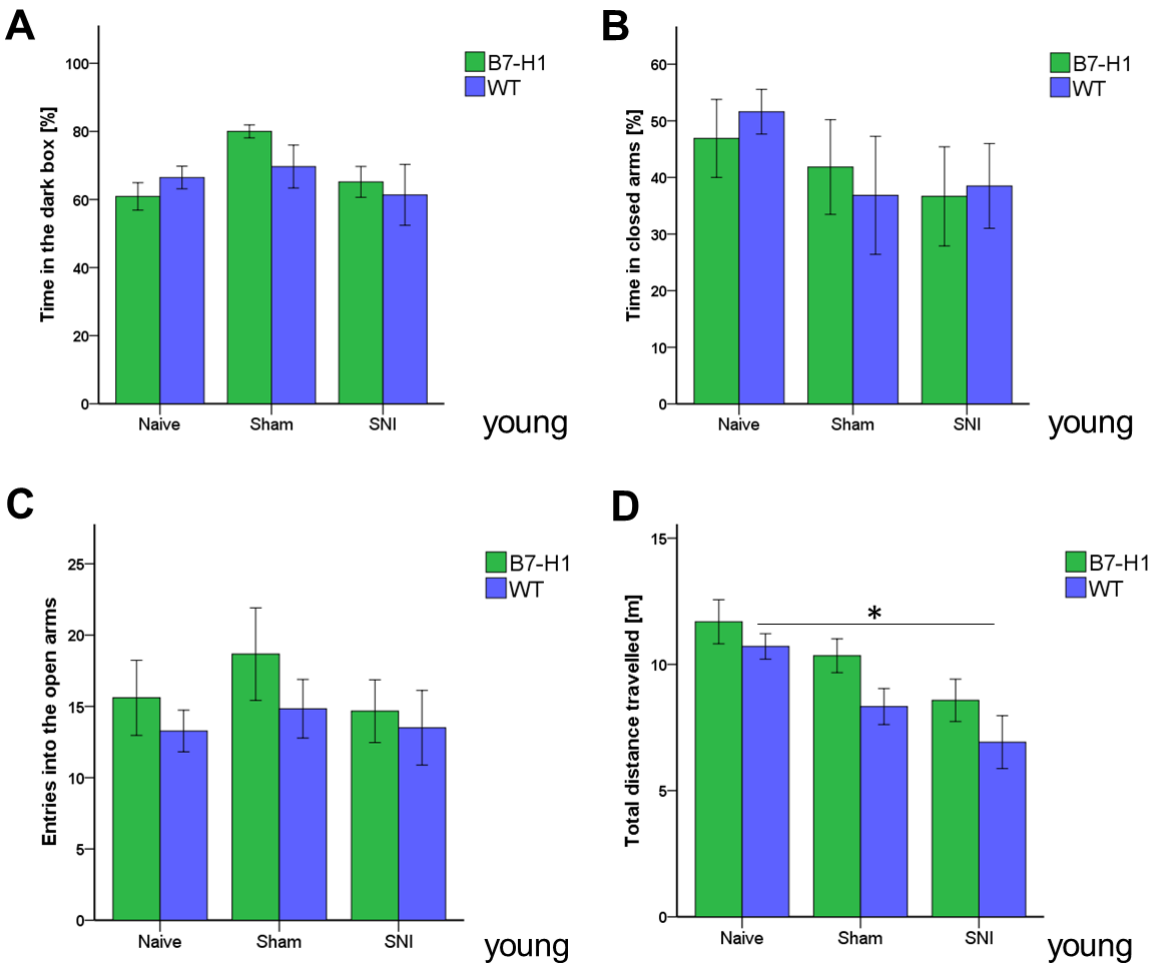

Figure 11: Anxiety-like behavior and locomotor activity in the elevated plus maze (EPM) and light-dark box (LDB). Bar graphs show the results of the EPM and LDB in young (8 weeks), male B7-H1 ko and wildtype littermates (WT), which were investigated in the naïve state, after sham surgery, and after spared nerve injury (SNI). No differences between genotypes or surgeries were found in the time spent in the dark box of the LDB (A), in the time spent in closed arms of the EPM (B), and in entries into open arms (C). WT mice travelled less compared to naïve mice after SNI ($p<0.05$ each), without intergroup difference (D).
B7-H1 ko: young (8 weeks, naïve: 11 male, SNI/sham: 6 male/ group).
WT: young (8 weeks, naïve: 11 male, SNI/sham: 6 male/ group).
*$p<0.05$.

Additionally, we performed the OF test for anxiety-like behavior, time spent in the center zone and total distance travelled did not differ between B7-H1 ko and WT mice, different age-groups, and at baseline or after surgery (Figure 12 A-C). Old naïve B7-H1 ko mice travelled a longer distance and achieved a higher average speed compared to WT mice ($p<0.05$ each, Figure 12 D, E),

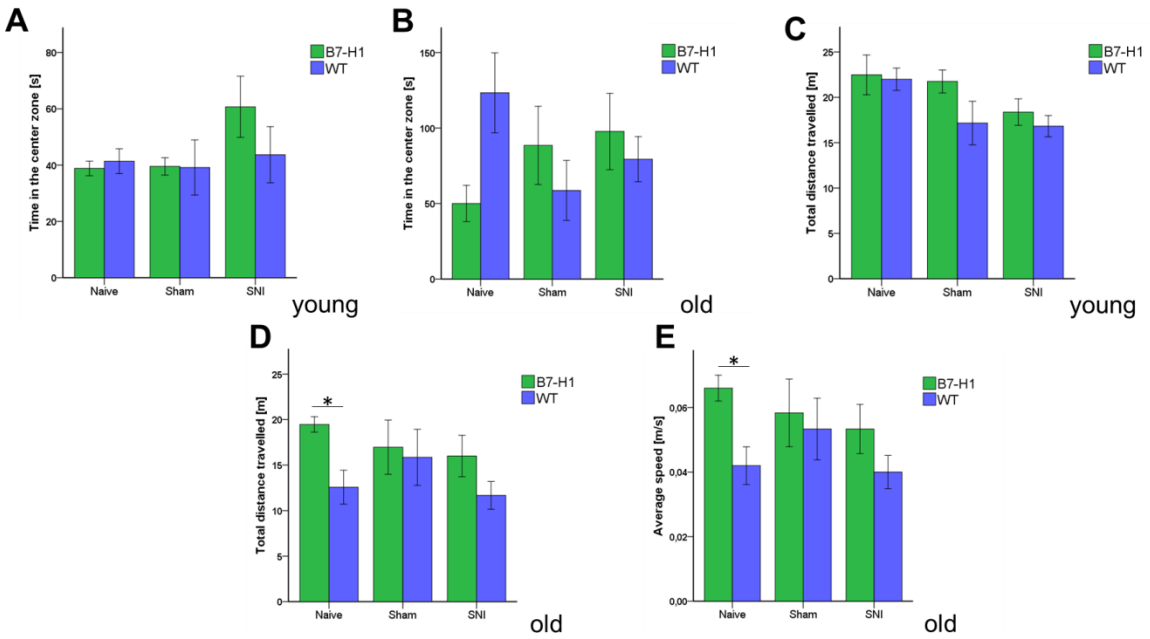

Figure 12: Anxiety-like behavior and locomotor activity in the open field (OF) test. Results of OF are shown in bar graphs. Male, young (8 weeks) and old (12 months) B7-H1 ko and wildtype littermates (WT) were investigated naïve, after sham surgery and after spared nerve injury (SNI). The time young (A) and old (B) mice spent in the center zone and in the total distance young mice travelled (C) did not differ between genotypes and surgeries. (D) Old, naïve B7-H1 ko mice travelled longer distance compared to WT mice. (E) The average speed was higher in old, naive B7-H1 ko mice compared to old, naïve WT mice.
B7-H1 ko: young (8 weeks, naïve: 11 male, SNI/sham: 6 male/group) and old (12 months, 6 male).
WT: young (8 weeks, naïve: 11 male, SNI/sham: 6 male/group) and old (12 months, 6 male).
*p<0.05.

In the FST, young and old B7-H1 mice did not differ in time spent immobile in the naïve state or after surgery compared to WT mice (Figure 13), showing no indication of depression-like behavior.

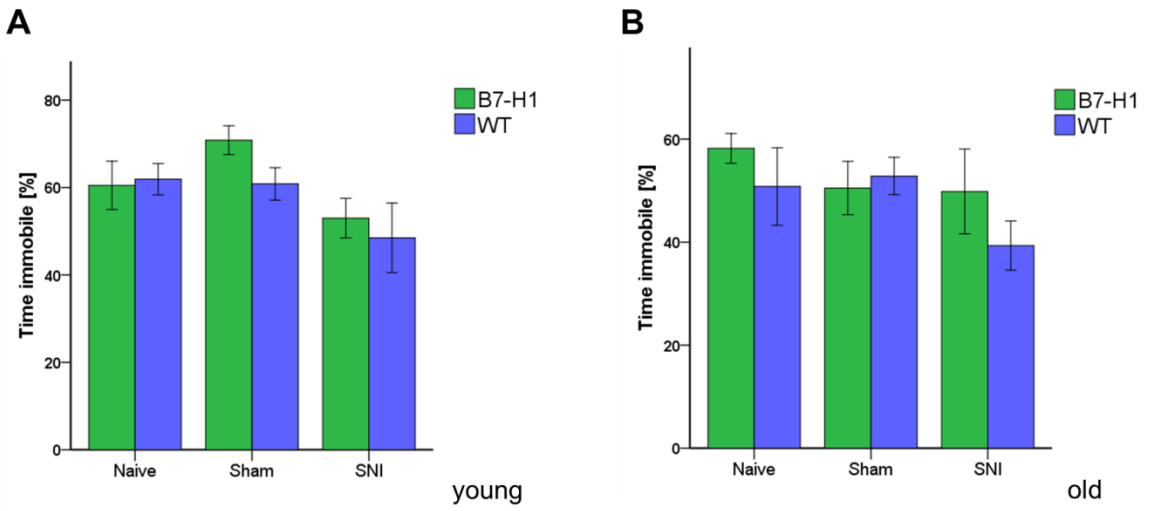

Figure 13: Depression-like behavior in the forced swim test (FST). The results of depression-like behavior in the forced swim test in young (8 weeks) and old (12 months), male B7-H1 ko and wildtype littermates (WT), naïve, after sham surgery and after spared nerve injury (SNI) is shown in bar graphs. No differences in time spent immobile were found in young (A) and old (B) mice between genotypes. Even after SNI both age-groups did not show differences compared to naïve mice.
B7-H1 ko: young (8 weeks, naïve: 11 male, SNI/sham: 6 male/group) and old (12 months, 6 male).
WT: young (8 weeks, naïve: 11 male, SNI/sham: 6 male/group) and old (12 months, 6 male).

5.3 No influence of pain on learning behavior and memory

In both genotypes and age-groups, the time mice swam until they reached the invisible platform during the MWM training days was similar and did not change after SNI. Also, the test duration, which decreased over time, did not differ between genotypes and age-groups (Figure 14)**,** being an indication of a comparable learning behavior.

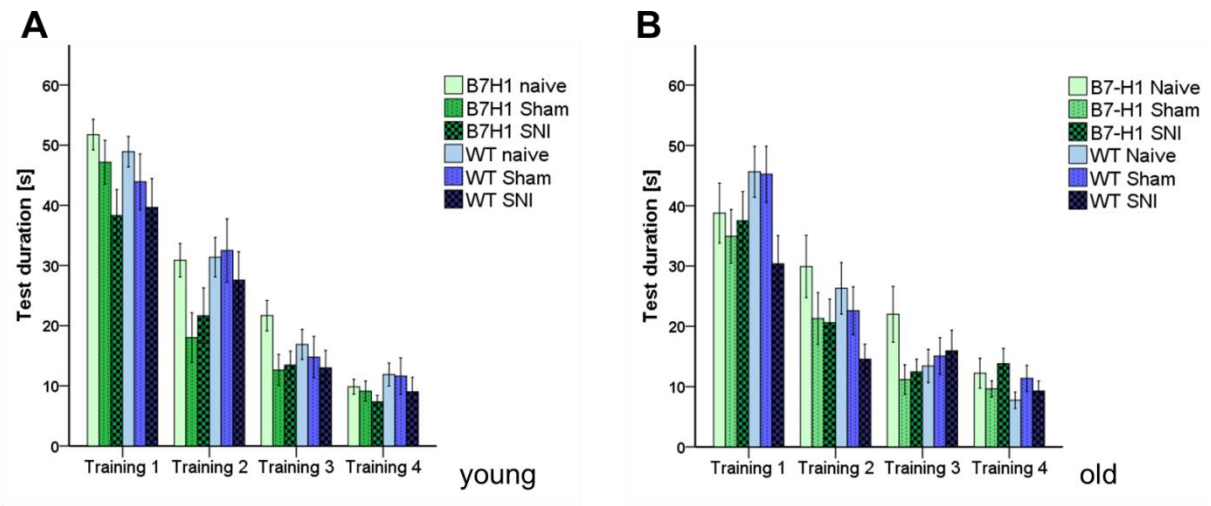

Figure 14: Cognitive behavior in the Morris water maze (MWM). Bar graphs show the results of the MWM training days in young (8 weeks) and old (12 months), naïve, sham or SNI treated B7-H1 ko and wildtype littermates (WT). Mice were testes on 4 consecutive days. Time mice needed to reach the hidden platform did not differ between genotypes and surgery in young (A) and old (B) mice.
B7-H1 ko: young (8 weeks, naïve: 11 male, SNI/sham: 6 male/group) and old (12 months, 6 male).
WT: young (8 weeks, naïve: 11 male, SNI/sham: 6 male/group) and old (12 months, 6 male).

No differences were found between genotypes and age-groups in time spent swimming in the target quadrant (Figure 15 A, B) and the total distance swum by young mice of both genotypes before and after surgery (Figure 15 C). Old B7-H1 mice in the naïve state swam shorter distances than their WT controls ($p<0.05$, Figure 15 D), while both genotypes displayed a further decrease in swimming distance after SNI ($p<0.05$ each, Figure 15 D). Young B7-H1 ko and WT mice did not differ in swimming velocity before and after SNI (Figure 15 E), whereas old naïve B7-H1 mice swam slower than their WT littermates ($p<0.05$), however, further decrease in average swimming speed after SNI was similar in both genotypes ($p<0.05$ each, Figure 15F).

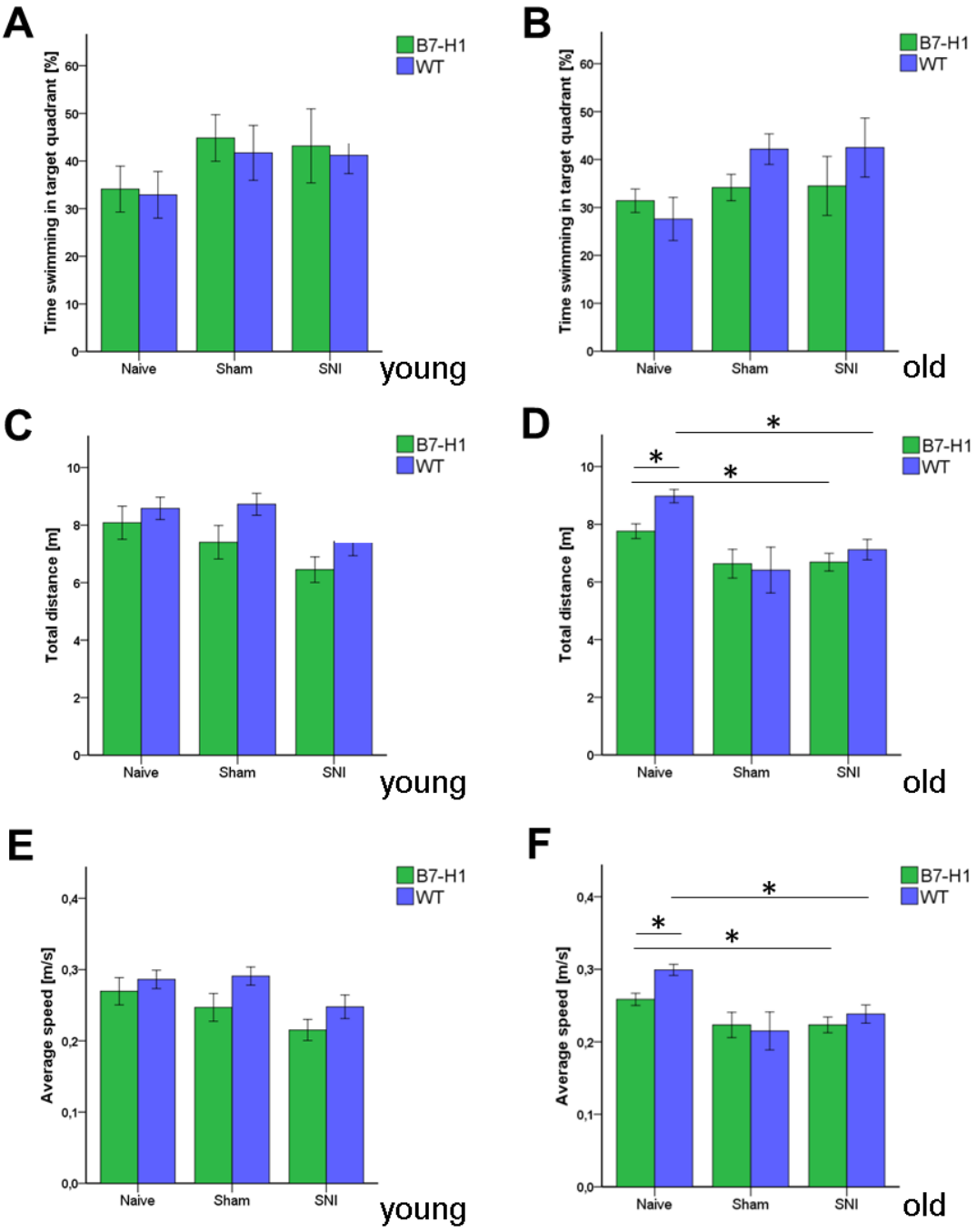

Figure 15: Memory and locomotor impairment in Morris water maze probe trail (MWM PT). Bar graphs show the results MWM PT in young (8 weeks) and old (12 months) B7-H1 ko and wildtype littermates (WT). Mice were investigated in the naïve state, after sham and after spared nerve injury (SNI). Time travelled in the target quadrant did not differ between genotypes and surgery of young (A) and old mice (B). (C) No difference in total distance travelled was detected between B7-H1 ko and WT mice in the naïve state or after SNI. (D) Old, naïve B7-H1 ko mice travelled less compared to WT mice ($p<0.05$). After SNI, the total distance travelled was shorter in both genotypes ($p<0.05$ each). (E) The Average speed did not differ in young mice between genotypes and surgeries. (F) Average speed of naïve, old B7-H1 ko mice were lower compared to naïve WT mice ($p<0.05$). After SNI, the average speed of B7-H1 ko and WT mice were lower compared to naïve mice ($p<0.05$).
B7-H1 ko: young (8 weeks, 6 male) and old (12 months, 6 male).
WT: young (8 weeks, 6 male) and old (12 months, 6 male).
*$p<0.05$.

5.4 Increase of miR-21 expression seven days after SNI in the injured tibial and common peroneal nerve of B7-H1 ko and WT mice

At baseline miR-21 expression levels did not show any difference in the tibial and common peroneal nerves of naïve B7-H1 ko and their WT littermates. In both genotypes miR-21 levels were elevated on day 7 after SNI without intergroup difference ($p<0.01$ each, Figure 16). Also on day 15 after SNI miR-21 expression was increased in both genotypes ($p<0.01$ each, old WT: $p<0.05$, Figure 16 A, B) except for young WT mice. miR-21 expression did not differ between B7-H1 ko and WT mice of all age-groups on day15 after SNI.

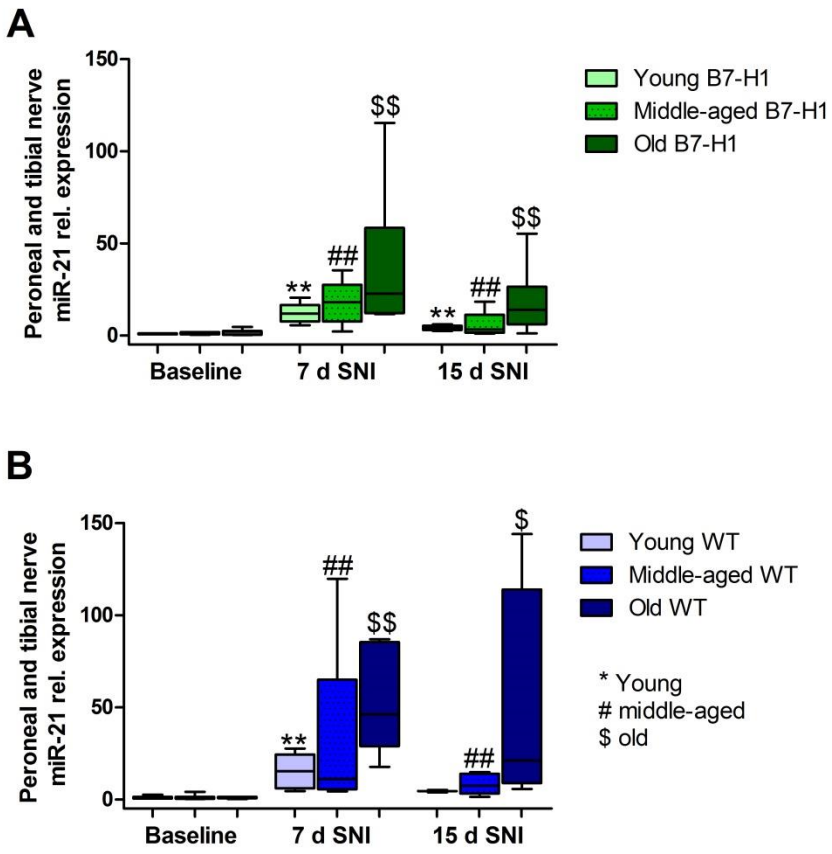

Figure 16: Relative gene expression of miR-21 in the tibial and common peroneal nerve. miR-21 relative expression as determined by quantitative real-time-PCR (qRT-PCR) in young (8 weeks), middle-aged (6 months) and old (12 months) B7-H1 ko and wildtype littermate (WT) mice at baseline, 7, and 15 days after SNI is shown in boxplots. (A) miR-21 expression was increased 7 days after SNI ($p<0.01$ each) in young, middle-aged and old B7-H1 ko mice. B7-H1 ko mice of all age-groups showed increased mir-21 expression levels 15 days ($p<0.01$ each) after SNI. (B) In young, middle-aged and old WT mice miR-21 levels were higher 7 ($p<0.01$ each) and 15 days (young/middle-aged: $p<0.01$, old: $p<0.05$) after SNI. Data were normalized to naïve WT mice.
B7-H1 ko: young (naïve, n= 6; 7d SNI, n= 6; 15 d SNI, n= 6), middle-aged (naïve, n= 6; 7d SNI, n= 6; 15 d SNI, n= 6), old (naïve, n= 7; 7d SNI, n= 6; 15 d SNI, n= 8)

WT: young (naïve, n= 6; 7d SNI, n= 6; 15 d SNI, n= 2), middle-aged (naïve, n= 6; 7d SNI, n= 6; 15 d SNI, n= 6), old (naïve, n= 6; 7d SNI, n= 6; 15 d SNI, n= 4).
$ p<0.05; **, ##, $$ p<0.01.

5.5 miR-21 is upregulated only in the uninjured sural nerve of WT mice after SNI

In the sural nerve of naïve, young B7-H1 ko, and WT mice miR-21 expression levels did not differ between genotypes at baseline and did not change after surgery (Figure 17 A). In middle-aged B7-H1 ko mice miR-21 baseline expression was three-fold higher in the sural nerve compared to WT mice ($p<0.05$) which did not change after surgery (Figure 17 A, B), whereas miR-21 expression was elevated on day 7 and 15 after SNI in middle-aged WT mice ($p<0.01$ each, Figure 17 B). miR-21 expression of old B7-H1 mice in the naïve state was not different from WT littermates and did not change after SNI, however, on day 7 after SNI miR-21 expression was increased in WT mice ($p<0.01$) and similarly showed higher miR-21 values on day 15 after surgery compared to baseline expression levels ($p<0.05$, Figure 17 A, B). Except for middle-aged WT mice showing elevated miR-21 expression levels compared to B7-H1 mice 7 days after SNI ($p<0.01$), no differences between genotypes of any age-group was detected. In summary miR-21 expression is increased after SNI in the uninjured sural nerve of WT mice, whereas B7-H1 ko mice seem to be spared.

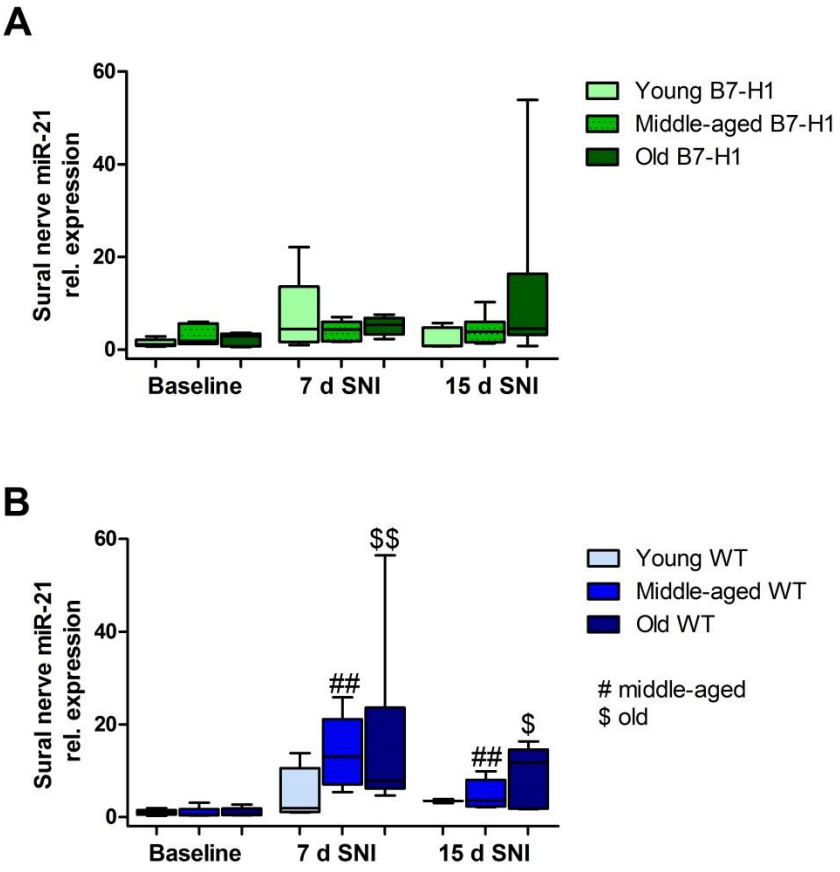

Figure 17: Relative gene expression of miR-21 in sural nerve. miR-21 relative expression as revealed by quantitative real-time-PCR (qRT-PCR) in young (8 weeks), middle-aged (6 months) and old (12 months) B7-H1 ko and wildtype littermate (WT) mice at baseline, 7, and 15 days after SNI is shown in boxplots. (A) 7 and 15 days after SNI no changes in miR-21 expression levels were detected in young, middle-aged and old B7-H1 ko mice. In the sural nerve of middle-aged B7-H1 ko mice miR-21 baseline expression level was higher compared to WT mice ($p<0.05$). (B) miR-21 was increased 7 ($p<0.01$ each) and 15 (middle-age: $p<0.01$, old $p<0.05$) days after SNI in the sural nerve of middle-aged and old WT mice. Data were normalized to naive WT mice.
B7-H1 ko: young (naïve, n= 6; 7d SNI, n= 5; 15 d SNI, n= 6), middle-aged (naïve, n= 6; 7d SNI, n= 5; 15 d SNI, n= 6), old (naïve, n= 7; 7d SNI, n= 6; 15 d SNI, n= 8)
WT: young (naïve, n= 6; 7d SNI, n= 2; 15 d SNI, n= 2), middle-aged (naïve, n= 6; 7d SNI, n= 6; 15 d SNI, n= 6), old (naïve, n= 6; 7d SNI, n= 6; 15 d SNI, n= 5).
$ $p<0.05$; ##, $$ $p<0.01$.

5.6 No alteration of miR-21 expression in DRG and WBC after SNI

In the L4 and L5 DRG, miR-21 expression levels were not different between naïve B7-H1 ko and WT mice at baseline and 7 and 15 days after surgery for all age-groups (Figure 18).

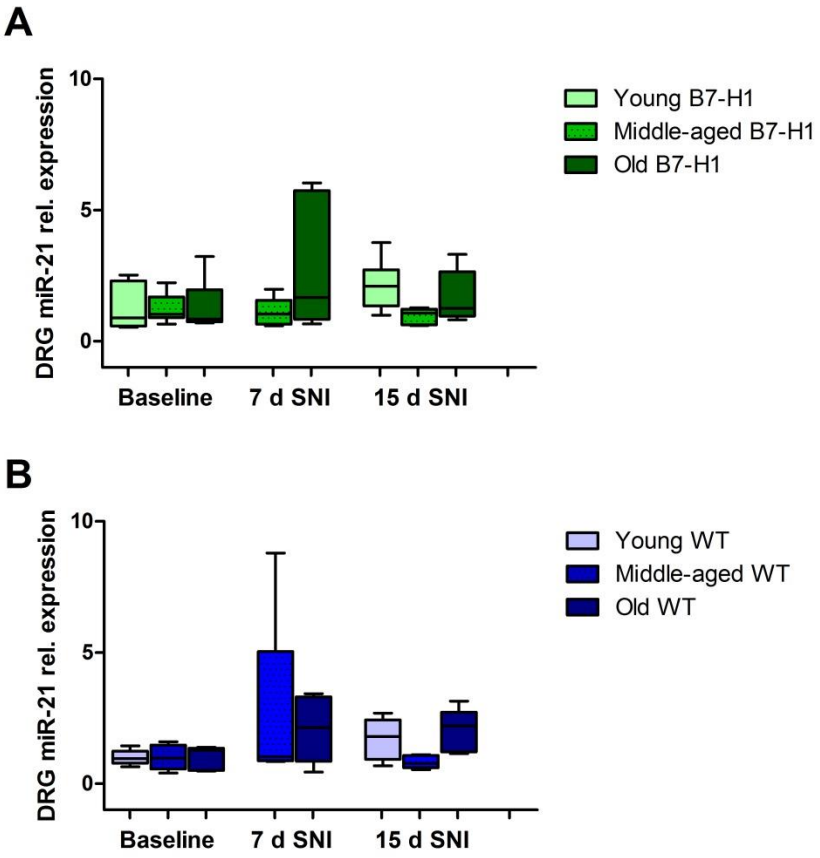

Figure 18: Relative gene expression of miR-21 in the dorsal root ganglia (DRG). miR-21 relative expression as measured by quantitative real-time-PCR (qRT-PCR) in young (8 weeks), middle-aged (6 months) and old (12 months) B7-H1 ko and wildtype littermate (WT) mice at baseline, 7, and 15 days after SNI are shown in boxplots. (A) No difference in miR-21 relative expression was detected 7 and 15 days after SNI in young, middle-aged and old B7-H1 ko mice. (B) 7 and 15 days after SNI WT mice of all ages did not show changes in miR-21 expression levels. Data were normalized to naive WT mice.
B7-H1 ko: young (naïve, n= 6; 7d SNI, n= 6; 15 d SNI, n= 6), middle-aged (naïve, n= 6; 7d SNI, n= 6; 15 d SNI, n= 6), old (naïve, n= 7; 7d SNI, n= 6; 15 d SNI, n= 8)
WT: young (naïve, n= 6; 7d SNI, n= 6; 15 d SNI, n= 6), middle-aged (naïve, n= 6; 7d SNI, n= 6; 15 d SNI, n= 6), old (naïve, n= 5; 7d SNI, n= 5; 15 d SNI, n= 5).

Similarly, systemic miR-21 expression in WBC was not different between genotypes at baseline and 7 days after sham and SNI surgery (Figure 19).

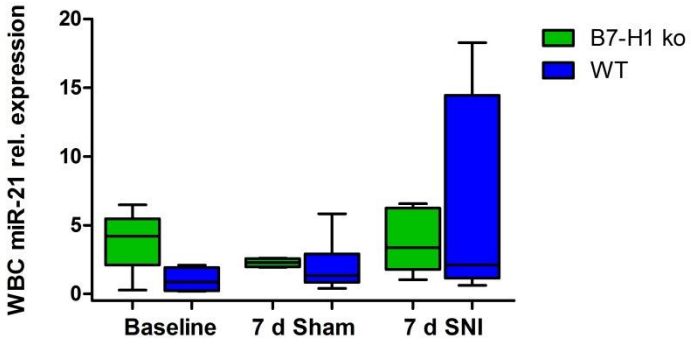

Figure 19: Relative gene expression of miR-21 in white blood cells (WBC). Boxplots show the miR-21 relative expression as revealed by quantitative real-time-PCR (qRT-PCR) in young (8 weeks) B7-H1 ko and wildtype littermate (WT) mice at baseline, 7 days after sham and SNI surgery. There was no change in miR-21 relative expression after sham and SNI treatment in the WBCs of B7-H1 ko and WT mice. Data were normalized to naive WT mice.
B7-H1 ko: naïve (n= 6), 7d sham (n= 8), 7d SNI (n= 4)
WT: naïve (n= 4), 7d sham (n= 9), 7d SNI (n= 9).

5.7 SNI-induced mechanical and heat hypersensitivity is reversed by perineurial miR-21 inhibitor injection

Perineurial injections of an LNA based miR-21 inhibitor were started at day three after surgery when mechanical and heat hypersensitivity were already present as shown in Figure 8 and 9. Mechanical hypersensitivity was reduced in B7-H1 ko (4-7 days after SNI: $p<0.01$) and WT mice (3 days after SNI: $p<0.05$; 4-7 days after SNI: $p<0.01$) compared to Scr treated B7-H1 ko and WT mice (Figure 20 A). Both genotypes showed mechanical hypersensitivity 4 days after the last miR-21 inhibitor injection, without intergroup differences. Thermal withdrawal latencies in miR-21 inhibitor treated B7-H1 ko (3-5 days after SNI: $p<0.01$; 6-7 days after SNI: $p<0.05$) and WT mice (4, 5, 7 days after SNI: $p<0.01$; 6 days after SNI: $p<0.05$) were increased compared to Scr treated mice, without differences between genotypes (Figure 20 B). Both genotypes showed hypersensitivity to heat stimuli 4 days after the last injection of the miR-21 inhibitor, without intergroup differences.

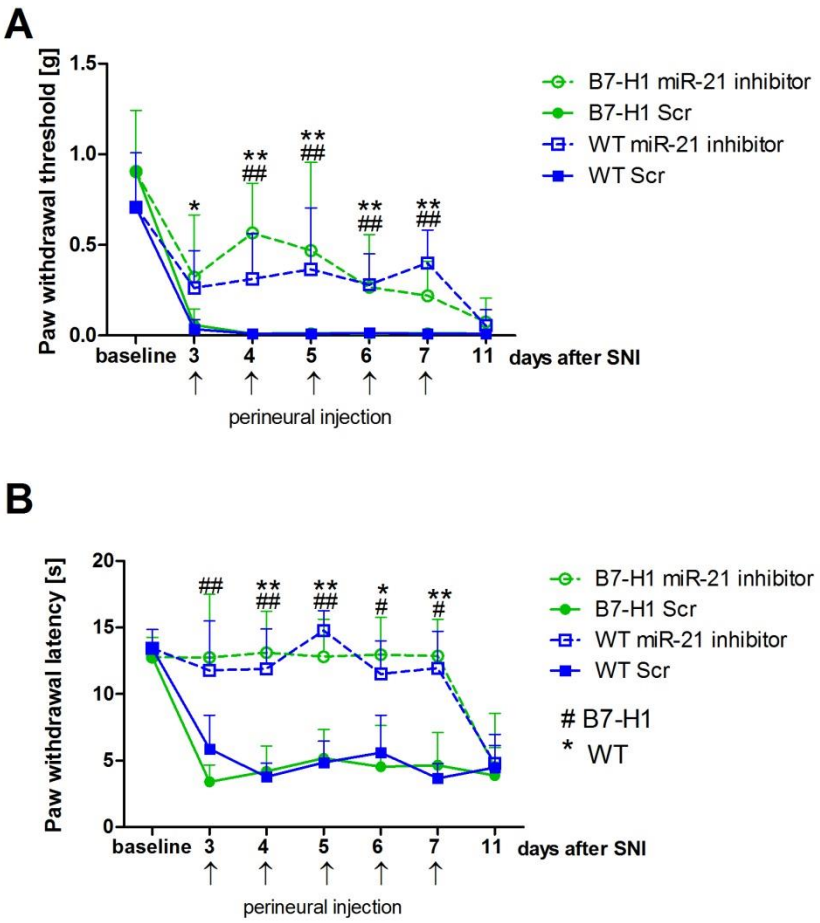

Figure 20: Paw withdrawal thresholds to mechanical and paw withdrawal latencies to thermal stimulation after perineurial injection of miR-21 inhibitor. Line charts show the results of the von-Frey and Hargreaves test in old (12 months) B7-H1 ko and wildtype littermate (WT) mice at baseline and after perineurial injection of miR-21 inhibitor on day 3-7 (indicated by the black arrows) after spared nerve injury (SNI). (A) miR-21 antagonism reverses mechanical hypersensitivity in B7-H1 ko (4-7 days after SNI: $p<0.01$) and WT mice (3 days after SNI: $p<0.05$; 4-7 days after SNI: $p<0.01$), without intergroup differences. (B) Perineurial injection of miRNA-21 inhibitor alleviates thermal hypersensitivity in B7-H1 ko (3-5 days after SNI: $p<0.01$; 6-7 days after SNI: $p<0.05$) and WT mice (4, 5, 7 days after SNI: $p<0.01$; 6 days after SNI: $p<0.05$) without differences between genotypes.
B7-H1 ko: old (12 months; miR-21 inhibitor: 5 male; Scr: 5 male)
WT: old (12 months; miR-21 inhibitor: 5 male; Scr: 2 male, 3 female)
*, ## $p<0.05$; **, ## $p<0.01$.
.

5.8 Invasion of macrophages and T cells into the injured peroneal and tibial nerves induced by SNI

Immunohistochemical stainings with antibodies against CD11b for the detection of macrophages (Figure 21) in the tibial and common peroneal nerve of young B7-H1 ko and WT mice showed an increased number of macrophages 7 days after SNI in

the tibial and common peroneal nerves of B7-H1 ko mice ($p<0.01$), while WT mice only displayed a trend to higher numbers of macrophages (Figure 23 A).

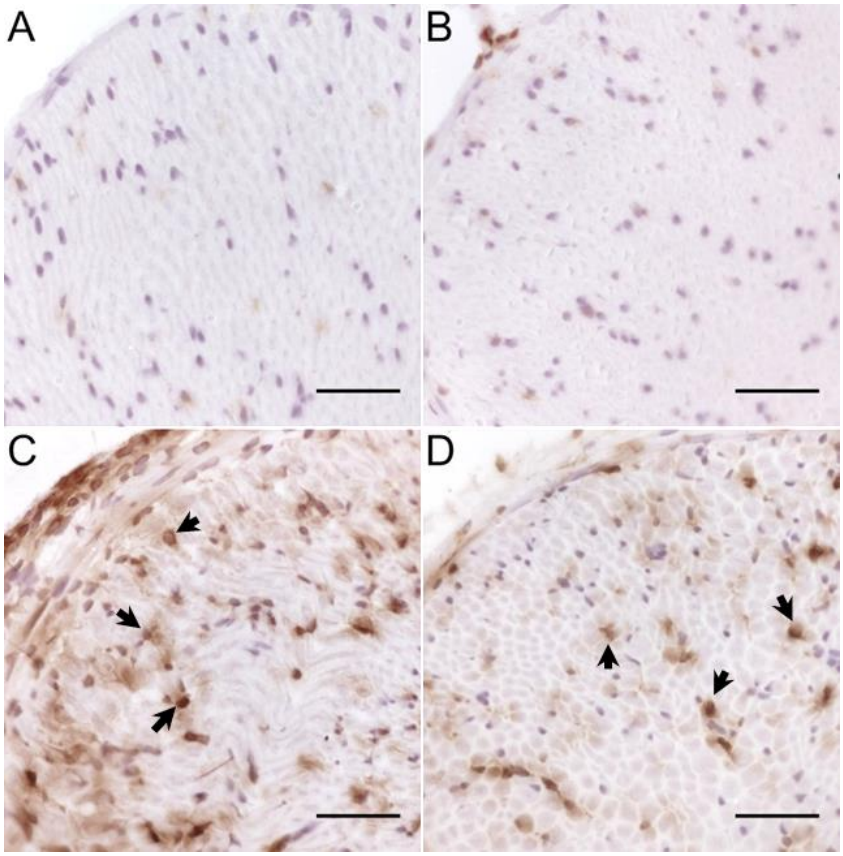

Figure 21: Representative photomicrographs of immunostainings against CD11b of frozen sections of the peroneal and tibial nerve. Antibodies against CD11b were used for the detection of macrophages in young, naive B7-H1 ko (A) and wildtype (WT) (B) mice, and 7 days after spared nerve injury (SNI). 7 days after SNI immunoreactivity (arrows) for macrophages was increased in B7-H1 ko (C) and WT (D) mice. Scale bar represents 50 µm.

In the tibial and common peroneal nerves of WT mice the number of T cells increased (Figure 22, $p<0.01$), whereas B7-H1 ko mice showed a clear trend to more T cells, which did not reach significance (Figure 23 C).

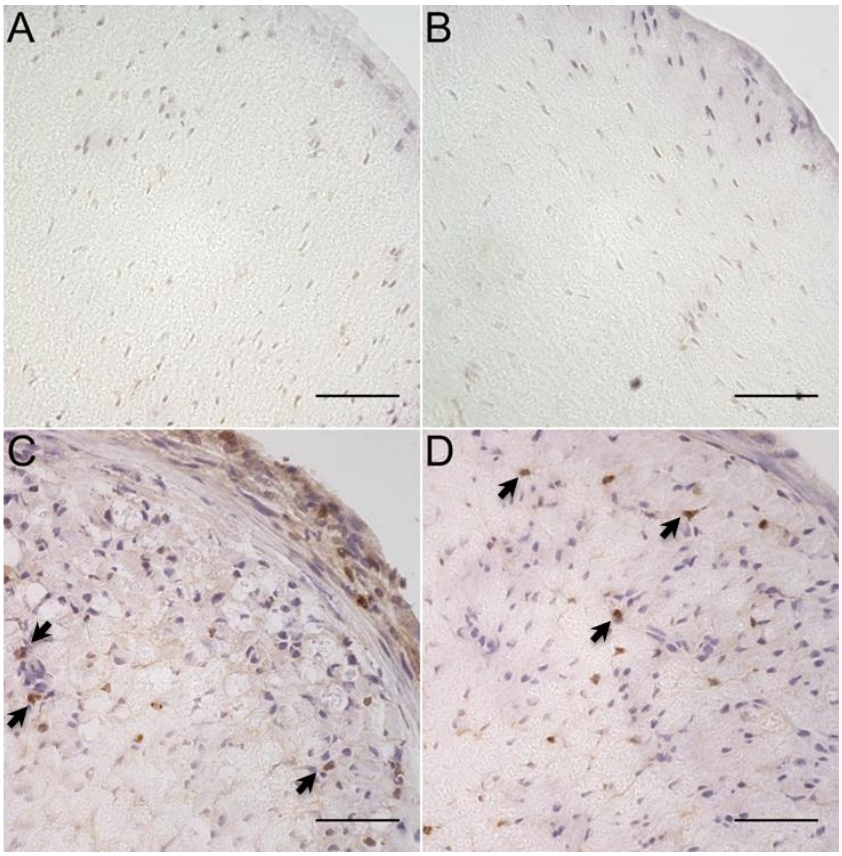

Figure 22: Representative photomicrographs of immunostainings against T cells of frozen sections of the peroneal and tibial nerve. Antibodies against CD3 were used for the detection of T cells in young, naive B7-H1 ko (A) and wildtype (WT) (B) mice, and 7 days after spared nerve injury (SNI). 7 days after SNI immunoreactivity (arrows) for T cells was enhanced in B7-H1 ko (C) and WT (D) mice. Scale bar represents 50 µm.

No differences were detected in the number of macrophages and T cells in the uninjured sural nerve when comparing B7-H1 ko and WT littermates in the naïve state and seven days after SNI (Figure 23 B, D).

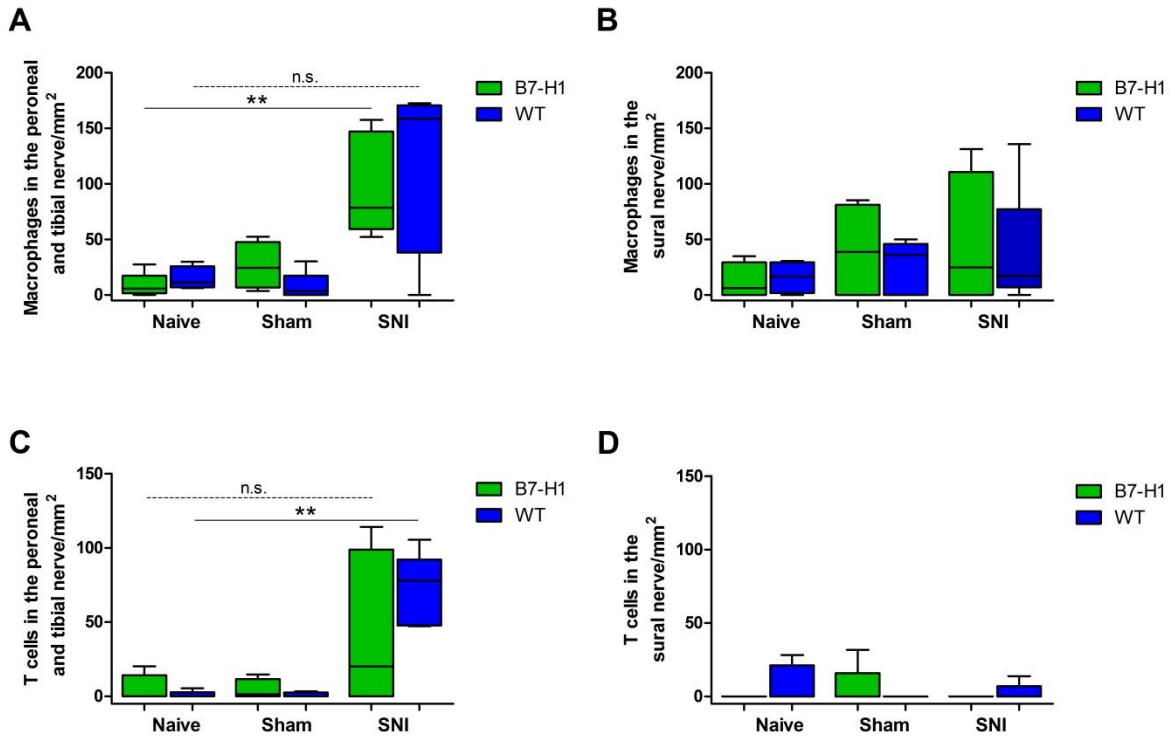

Figure 23: Quantification of the immunohistochemical staining of CD11b for the detection of macrophages and for the detection of T cells (CD3). (A) The number of macrophages in the tibial and common peroneal nerve of B7-H1 ko mice was increased compared to naïve mice ($p<0.01$). (B) After SNI the number of macrophages in the sural nerve did not differ between B7-H1 ko and WT mice. (C) WT mice showed increased number of T cells in the tibial and common peroneal nerve after SNI ($p<0.01$). (D) After SNI, no changes in number of T cells in the sural nerve of B7-H1 ko and WT mice compared to naïve mice were found.
B7-H1 ko: young (8 weeks; naïve: 2 male, 3 female; sham: 3 male, 2 female; SNI: 5 male)
WT: young (8 weeks; naïve: 3 male, 2 female; sham: 4 male, 1 female; SNI: 5 female)
**$p<0.01$; n.s. not significant

5.9 No differences in miR-21 expression in WBC of C57BL/6 mice after SNI

We investigated systemic miR-21 expression in WBC of two different C57BL/6 mouse strains (C57BL/6J and C57BL/6N). miR-21 expression was not different between both mouse strains at baseline and 7 days after sham and SNI surgery (Figure 24).

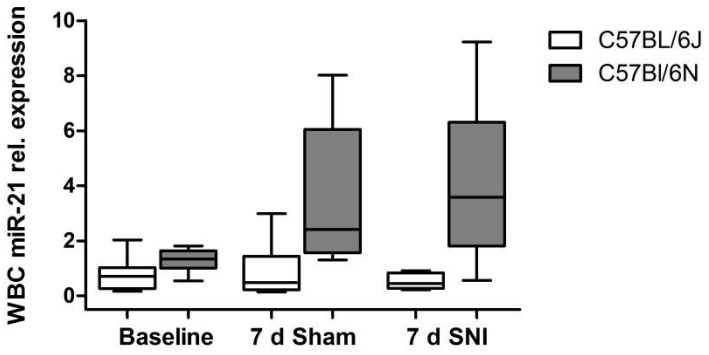

Figure 24: Relative gene expression of miR-21 in white blood cells (WBC). Boxplots show the miR-21 relative expression as revealed by quantitative real-time-PCR (qRT-PCR) in young (8 weeks) C57Bl/6J and C57Bl/6N mice at baseline, 7 days after SNI and sham surgery. There was no change in miR-21 relative expression after sham and SNI treatment in both mouse strains and no difference between both strains. Data were normalized to naive mice.
B7-H1 ko: naïve (n= 6), 7d sham (n= 8), 7d SNI (n= 4)
WT: naïve (n= 4), 7d sham (n= 9), 7d SNI (n= 9).

6 Discussion

Recent reports highlighted B7-H1 and miR-21 as potential key players in inflammation and neuropathic pain (Sheedy, 2015;Chen et al., 2017). We investigated the interplay between B7-H1 and miR-21 and demonstrate a potential link between miR-21 induction in the injured tibial and common peroneal nerves after SNI and pain behavior in the B7-H1 ko mouse.

An association between B7-H1 and pain behavior was described in a previous study (Üçeyler et al., 2010) with enhanced neural inflammation and sustained pain behavior after CCI in B7-H1 ko mice. Recently, Chen et al. reported B7-H1 as an important endogenous pain inhibitor demonstrating that intraplantar injections of B7-H1 attenuated chronic neuropathic pain, inflammatory pain, and also increased pain thresholds in naïve mice (Chen et al., 2017). To further characterize potential influences of the nervous and the immune system on the development and maintenance of pain and on affective and cognitive behavior, we applied the SNI model. SNI is a robust neuropathic pain model that leads to long lasting alterations in pain behavior (Decosterd and Woolf, 2000). Due to known changes in pain associated behavior in mice and rats with ageing, we examined several age-groups (Hess et al., 1981;Crisp et al., 2003;Lemmer et al., 2015;Üçeyler et al., 2016). At baseline we found mechanical hypersensitivity of young and middle-aged B7-H1 ko mice compared to their littermates. These results are in line with a previous study that also reported lower mechanical withdrawal thresholds in young B7-H1 ko mice (Üçeyler et al., 2010).

In the CCI model B7-H1 ko mice showed sustained mechanical hyperalgesia after surgery, whereas after SNI, B7-H1 ko and WT mice of all age-groups developed mechanical hypersensitivity in the sural nerve territory without differences between genotypes. This may be due to the fact that pain remains permanent after SNI (Decosterd and Woolf, 2000) and no recovery phase is reached in contrast to the CCI model, in which differences between genotypes were detectable. Furthermore, the investigated pain thresholds being near maximum might prevent the detection of small differences.

B7-H1 ko and WT mice also displayed heat hypersensitivity after SNI, which was not reported in the first description of this model (Decosterd and Woolf, 2000). However, the authors tested withdrawal latency and duration, and reported that thermal

responsiveness (hot and cold) was increased. In addition, Decosterd and Woolf investigated rats, whereas we tested mice, which is an important difference when assessing pain behavior (Yezierski, 2012). Nociception even differs in mice of different strains as already shown in 1999 by Mogil et al. by investigating eleven inbred mouse strains (Mogil et al., 1999). Importantly, studies performed in rats comparing SNI and CCI revealed thermal hyperalgesia in both models (Baliki et al., 2005;Mirzaei et al., 2008).

Anxiety, depression, and cognitive impairment are symptoms, which are often reported by patients suffering from chronic pain (Argoff, 2007;Moriarty et al., 2011). We therefore investigated affective, depression-like, and cognitive behavior in our mouse model in the naïve state, after sham surgery, and after SNI. We performed three different anxiety tests to cover different facets of affective behavior, since the intra-individual outcome variation is high in tests for anxiety-like behavior (Ramos, 2008). All three performed tests (OF, LDB, EPM) are exploration-based, but display a diversity in the environmental setting and are therefore appropriate tasks to assess affective behavior. We did not detect any influence of SNI on anxiety-like behavior in both genotypes and age-groups. Recent studies report increased anxiety-like behavior in mice 30 days after SNI in the LDB (Palazzo et al., 2016) and also increased anxiety behavior with ageing (Lamberty and Gower, 1993;Boguszewski and Zagrodzka, 2002), which may be explained by the later time points investigated and the usage of different mouse strains that markedly influence response to anxiety-inducing tests (O'Leary et al., 2013). Also, differences in housing, habituation, and handling may cause behavioral differences in rodents (Wilson and Mogil, 2001). We performed the MWM test, to assess the impact of neuropathic pain on cognitive behavior and memory performance. In the MWM training mice, treated with SNI, performed in the same manner as mice in the naïve state, or after sham surgery. Similarly, Leite-Almeida and colleagues showed that neuropathic pain has no influence on learning behavior in rats (Leite-Almeida et al., 2009). Also, we did not detect any difference of neuropathic pain on memory performance in the PT in both genotypes and age-groups, in contrast to another study that identified young mice to be better performers than old ones (Francia et al., 2006). This diversity of the influence of neuropathic pain on affective and cognitive behavior rather underlines the necessity to consider time points, species, and mouse strains carefully.

The treatment of chronic pain remains challenging and diagnostic biomarkers and better treatment possibilities are required. miRNA have first been described as potential biomarkers in different types of cancer, like B-cell lymphoma, pancreatic cancer, and gastric cancer (Volinia et al., 2006;Lawrie et al., 2007;Liu et al., 2011b). However, they have recently also been suggested as biomarkers in several neurological disorders like migraine, spinal cord injury, and Parkinson's disease (Andersen et al., 2016;Cosin-Tomas et al., 2016;Martirosyan et al., 2016). Since it is not understood, why individual patients are predisposed to developing neuropathic pain whereas others are spared, biomarkers for the identification of those patients, who are at risk would be useful. Being involved in cellular pathways underlying neuropathic pain, miRNA are promising candidates (Andersen et al., 2014). Besides the usage of miRNA as biomarkers, targeting or mimicking specific miRNA could be a potential strategy for treatment of neuropathic pain.

We investigated the role of miR-21 in the B7-H1 ko model, to gain new insights into their neuro-immune interaction and to assess their role in neuropathic pain. Iliopoulos and colleagues described miR-21 as a downstream target of the B7-H1 receptor PD-1. They demonstrated *in vitro* that the lack of PD-1 leads to enhanced binding of STAT5 in the promotor area of miR-21, which results in miR-21 upregulation. These results were confirmed in PD-1 ko mice, showing increased miR-21 expression in T cells compared to WT mice (Iliopoulos et al., 2011). Contrary to our expectation, the B7-H1 ko mouse did not show an upregulation of miR-21 in nervous tissue and might therefore not serve as a good model for miR-21 overexpression. One explanation could be that PD-1 has two ligands, B7-H1 and PD-L2 (Latchman et al., 2001). The second ligand PD-L2 might compensate the lack of B7-H1 and might adapt miR-21 regulation.

miR-21 has been described as a key mediator between pro- and anti-inflammatory conditions (Sheedy, 2015). Besides, miR-21 upregulation has also been described in several models of neuropathic pain. An upregulation of miR-21 was shown in DRG at different time points after sciatic nerve transection in mice and rats, in DRG after nerve ligation, and in the sciatic nerve after crush injury (Strickland et al., 2011;Wu et al., 2011;Yu et al., 2011;Hori et al., 2016). Additionally, Wu et al. reported that elements of the RISC complex and mRNA processing bodies (P-bodies), both components of miRNA biosynthesis, are upregulated after nerve injury, indicating a

role of miRNA pathways in peripheral nerve regeneration (Wu et al., 2011). Increased miR-21 expression has also been shown in the spinal cord 7 and 14 days after CCI using a TaqMan low density array (Genda et al., 2013) suggesting an involvement of miR-21 in neuropathic pain. Contrary to these results, a microarray analysis showed decreased miR-21 levels in circulating miRNA extracted from rat sera after SNL (Xu et al., 2014).

We report that miR-21 is upregulated in the injured tibial and common peroneal nerves of B7-H1 ko and WT mice after SNI treatment. In the uninjured sural nerve increased miR-21 expression is only present in middle-aged and old WT mice. This finding suggests that miR-21 upregulation is linked to the injured nerve and could also be related to inflammation. Since macrophages infiltrate the injured peripheral nerve and release cytokines and chemokines that play an important role in peripheral sensitization (Calvo et al., 2012), we hypothesize that immune cells may be the source of miR-21 (Figure 25).

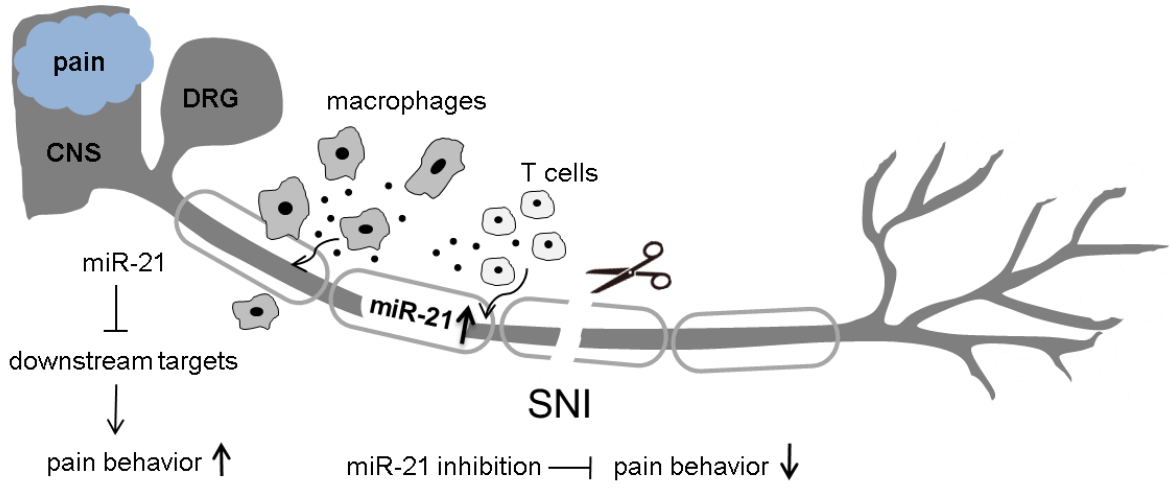

Figure 25: miR-21 as a potential mediator of neuropathic pain. After spared nerve injury (SNI) miR-21 expression changes might influence neuronal functions and pain behavior. miR-21 is upregulated in the injured nerve. Immune cells (macrophages and T cells) infiltrate the injured nerve and are potential sources of miR-21. Additionally, immune cells release pro-inflammatory mediators (e.g. cytokines and chemokines), which contribute to neuropathic pain. Several targets of miR-21 influence neuronal associated pathways, and their inhibition is leading to pain. Perineurial administration of miR-21 inhibitor alleviates pain.

Our results demonstrate that 7 days after SNI surgery, macrophages and T cells infiltrated the injured tibial and common peroneal nerves of young B7-H1 ko and WT mice, whereas no differences in the number of immune cells were detected in the spared sural nerve. Further research is needed to specify the localization of miR-21 in the axon after SNI. Performing in situ hybridization of miR-21 combined with

immunohistochemical stainings against immune cells, like macrophages or T cells could determine the source of miR-21. One further explanation for increased miR-21 expression in the nerve could be that miR-21 is produced by the somata in the DRG and is transported axonally as described for miRNA by other groups (Bicker et al., 2013;Ingoglia and Jalloh, 2016).

We showed that inhibition of miR-21 by perineurial administration of a LNA based miR-21 antagonist relieves pain behavior in B7-H1 ko and WT mice. These results are in line with studies in rats, showing alleviation of mechanical hypersensitivity after intrathecal administration of miR-21 inhibitor (Sakai and Suzuki, 2013).

miR-21 upregulation might lead to downregulation of multiple targets that are involved in analgesia. However, the precise mechanism connecting miR-21 and pain is not fully understood. There are only few targets, which have been described as being involved in nerve fiber sensitization and nerve regeneration. The tumor suppressor phosphatase and tensin homolog (PTEN) is one of these targets and has been described as miR-21 target in several studies. Huang and colleagues identified PTEN as an important mediator of nociceptive behavior in rats after CCI that causes neuroinflammation in astrocytes (Huang et al., 2015). Another study described that deletion of PTEN in Schwann cells of mice leads to a progressive peripheral neuropathy (Goebbels et al., 2012). In addition, PTEN is associated with neuron sprouting by enhancing adult peripheral axon outgrowth (Yu et al., 2011) and inhibits the production of TNF (Sheedy, 2015). Besides, there are further studies that characterized PTEN as an anti-inflammatory agent. Das et al. showed that downregulation of PTEN and programmed cell death 4 (PDCD4), a further miR-21 target gene, results in an enhanced production of the anti-inflammatory cytokine IL-10 (Das et al., 2014). Further targets of miR-21 are inhibitors of matrix metalloproteinases (e.g. RECK and TIMP3) (Gabriely et al., 2008). Matrix metalloproteinases have been shown to play a role in the development of neuropathic pain through interleukin-1β cleavage and microglia or astrocyte activation (Kawasaki et al., 2008). However further research is needed to identify additional downstream targets of miR-21 that play a role in pain pathways. One approach is to search for candidates with analgesic effect, like chemokines and cytokines, that are downregulated after SNI because of their translational inhibition by miR-21.

Due to the fact that miR-21 expression was not higher in B7-H1 ko mice and no differences in pain behavior were detected in B7-H1 ko mice compared to WT mice, the B7-H1 ko mouse may be of limited relevance for the investigation of miR-21 related neuropathic pain. However, this study supports miR-21 as a promising candidate to identify downstream targets that might reveal new therapeutic approaches for the treatment of neuropathic pain. Besides, our data emphasize the contribution of miRNA to the regulation of neuronal and immune processes that influence neuropathic pain.

7 References

Aboobaker, A.A., Tomancak, P., Patel, N., Rubin, G.M., and Lai, E.C. (2005). Drosophila microRNAs exhibit diverse spatial expression patterns during embryonic development. *Proc Natl Acad Sci U S A* 102**,** 18017-18022.

Aldrich, B.T., Frakes, E.P., Kasuya, J., Hammond, D.L., and Kitamoto, T. (2009). Changes in expression of sensory organ-specific microRNAs in rat dorsal root ganglia in association with mechanical hypersensitivity induced by spinal nerve ligation. *Neuroscience* 164**,** 711-723.

Andersen, H.H., Duroux, M., and Gazerani, P. (2014). MicroRNAs as modulators and biomarkers of inflammatory and neuropathic pain conditions. *Neurobiol Dis* 71**,** 159-168.

Andersen, H.H., Duroux, M., and Gazerani, P. (2016). Serum MicroRNA Signatures in Migraineurs During Attacks and in Pain-Free Periods. *Mol Neurobiol* 53**,** 1494-1500.

Argoff, C.E. (2007). The coexistence of neuropathic pain, sleep, and psychiatric disorders: a novel treatment approach. *Clin J Pain* 23**,** 15-22.

Attal, N., Lanteri-Minet, M., Laurent, B., Fermanian, J., and Bouhassira, D. (2011). The specific disease burden of neuropathic pain: results of a French nationwide survey. *Pain* 152**,** 2836-2843.

Bali, K.K., and Kuner, R. (2014). Noncoding RNAs: key molecules in understanding and treating pain. *Trends Mol Med* 20**,** 437-448.

Baliki, M., Calvo, O., Chialvo, D.R., and Apkarian, A.V. (2005). Spared nerve injury rats exhibit thermal hyperalgesia on an automated operant dynamic thermal escape task. *Mol Pain* 1**,** 18.

Baron, R., Binder, A., and Wasner, G. (2010). Neuropathic pain: diagnosis, pathophysiological mechanisms, and treatment. *Lancet Neurol* 9**,** 807-819.

Baron, R., Hans, G., and Dickenson, A.H. (2013). Peripheral input and its importance for central sensitization. *Ann Neurol* 74**,** 630-636.

Basbaum, A.I., Bautista, D.M., Scherrer, G., and Julius, D. (2009). Cellular and Molecular Mechanisms of Pain. *Cell* 139**,** 267-284.

Bennett, G.J., and Xie, Y.K. (1988). A peripheral mononeuropathy in rat that produces disorders of pain sensation like those seen in man. *Pain* 33**,** 87-107.

Bicker, S., Khudayberdiev, S., Weiss, K., Zocher, K., Baumeister, S., and Schratt, G. (2013). The DEAH-box helicase DHX36 mediates dendritic localization of the neuronal precursor-microRNA-134. *Genes Dev* 27**,** 991-996.

Bjersing, J.L., Bokarewa, M.I., and Mannerkorpi, K. (2015). Profile of circulating microRNAs in fibromyalgia and their relation to symptom severity: an exploratory study. *Rheumatol Int* 35**,** 635-642.

Blyth, F.M., March, L.M., Nicholas, M.K., and Cousins, M.J. (2003). Chronic pain, work performance and litigation. *Pain* 103**,** 41-47.

Bodhankar, S., Galipeau, D., Vandenbark, A.A., and Offner, H. (2013). PD-1 Interaction with PD-L1 but not PD-L2 on B-cells Mediates Protective Effects of Estrogen against EAE. *J Clin Cell Immunol* 4**,** 143.

Boguszewski, P., and Zagrodzka, J. (2002). Emotional changes related to age in rats--a behavioral analysis. *Behav Brain Res* 133**,** 323-332.

Bouchie, A. (2013). First microRNA mimic enters clinic. *Nat Biotechnol* 31**,** 577.

Bouhassira, D., Lanteri-Minet, M., Attal, N., Laurent, B., and Touboul, C. (2008). Prevalence of chronic pain with neuropathic characteristics in the general population. *Pain* 136**,** 380-387.

Boussiotis, V.A. (2016). Molecular and Biochemical Aspects of the PD-1 Checkpoint Pathway. *N Engl J Med* 375**,** 1767-1778.
Brenner, D.S., Golden, J.P., and Gereau, R.W.T. (2012). A novel behavioral assay for measuring cold sensation in mice. *PLoS One* 7**,** e39765.
Calin, G.A., Sevignani, C., Dumitru, C.D., Hyslop, T., Noch, E., Yendamuri, S., Shimizu, M., Rattan, S., Bullrich, F., Negrini, M., and Croce, C.M. (2004). Human microRNA genes are frequently located at fragile sites and genomic regions involved in cancers. *Proc Natl Acad Sci U S A* 101**,** 2999-3004.
Calvo, M., Dawes, J.M., and Bennett, D.L. (2012). The role of the immune system in the generation of neuropathic pain. *Lancet Neurol* 11**,** 629-642.
Caterina, M.J., Schumacher, M.A., Tominaga, M., Rosen, T.A., Levine, J.D., and Julius, D. (1997). The capsaicin receptor: a heat-activated ion channel in the pain pathway. *Nature* 389**,** 816-824.
Cerda-Olmedo, G., Mena-Duran, A.V., Monsalve, V., and Oltra, E. (2015). Identification of a microRNA signature for the diagnosis of fibromyalgia. *PLoS One* 10**,** e0121903.
Chen, G., Kim, Y.H., Li, H., Luo, H., Liu, D.L., Zhang, Z.J., Lay, M., Chang, W., Zhang, Y.Q., and Ji, R.R. (2017). PD-L1 inhibits acute and chronic pain by suppressing nociceptive neuron activity via PD-1. *Nat Neurosci*.
Colloca, L., Ludman, T., Bouhassira, D., Baron, R., Dickenson, A.H., Yarnitsky, D., Freeman, R., Truini, A., Attal, N., Finnerup, N.B., Eccleston, C., Kalso, E., Bennett, D.L., Dworkin, R.H., and Raja, S.N. (2017). Neuropathic pain. *Nat Rev Dis Primers* 3**,** 17002.
Cosin-Tomas, M., Antonell, A., Llado, A., Alcolea, D., Fortea, J., Ezquerra, M., Lleo, A., Marti, M.J., Pallas, M., Sanchez-Valle, R., Molinuevo, J.L., Sanfeliu, C., and Kaliman, P. (2016). Plasma miR-34a-5p and miR-545-3p as Early Biomarkers of Alzheimer's Disease: Potential and Limitations. *Mol Neurobiol*.
Coyle, A.J., and Gutierrez-Ramos, J.C. (2001). The expanding B7 superfamily: increasing complexity in costimulatory signals regulating T cell function. *Nat Immunol* 2**,** 203-209.
Crawley, J., and Goodwin, F.K. (1980). Preliminary report of a simple animal behavior model for the anxiolytic effects of benzodiazepines. *Pharmacol Biochem Behav* 13**,** 167-170.
Crisp, T., Giles, J.R., Cruce, W.L., Mcburney, D.L., and Stuesse, S.L. (2003). The effects of aging on thermal hyperalgesia and tactile-evoked allodynia using two models of peripheral mononeuropathy in the rat. *Neurosci Lett* 339**,** 103-106.
Cunha, F.Q., Poole, S., Lorenzetti, B.B., Veiga, F.H., and Ferreira, S.H. (1999). Cytokine-mediated inflammatory hyperalgesia limited by interleukin-4. *Br J Pharmacol* 126**,** 45-50.
Das, A., Ganesh, K., Khanna, S., Sen, C.K., and Roy, S. (2014). Engulfment of apoptotic cells by macrophages: a role of microRNA-21 in the resolution of wound inflammation. *J Immunol* 192**,** 1120-1129.
Davis, J.B., Gray, J., Gunthorpe, M.J., Hatcher, J.P., Davey, P.T., Overend, P., Harries, M.H., Latcham, J., Clapham, C., Atkinson, K., Hughes, S.A., Rance, K., Grau, E., Harper, A.J., Pugh, P.L., Rogers, D.C., Bingham, S., Randall, A., and Sheardown, S.A. (2000). Vanilloid receptor-1 is essential for inflammatory thermal hyperalgesia. *Nature* 405**,** 183-187.
Decosterd, I., and Woolf, C.J. (2000). Spared nerve injury: an animal model of persistent peripheral neuropathic pain. *Pain* 87**,** 149-158.

Dib-Hajj, S.D., Geha, P., and Waxman, S.G. (2017). Sodium channels in pain disorders: pathophysiology and prospects for treatment. *Pain* 158 Suppl 1**,** S97-S107.

Dong, H., Strome, S.E., Salomao, D.R., Tamura, H., Hirano, F., Flies, D.B., Roche, P.C., Lu, J., Zhu, G., Tamada, K., Lennon, V.A., Celis, E., and Chen, L. (2002). Tumor-associated B7-H1 promotes T-cell apoptosis: a potential mechanism of immune evasion. *Nat Med* 8**,** 793-800.

Dong, H., Zhu, G., Tamada, K., and Chen, L. (1999). B7-H1, a third member of the B7 family, co-stimulates T-cell proliferation and interleukin-10 secretion. *Nat Med* 5**,** 1365-1369.

Dong, H., Zhu, G., Tamada, K., Flies, D.B., Van Deursen, J.M., and Chen, L. (2004). B7-H1 determines accumulation and deletion of intrahepatic CD8(+) T lymphocytes. *Immunity* 20**,** 327-336.

Dong, X., Han, S., Zylka, M.J., Simon, M.I., and Anderson, D.J. (2001). A diverse family of GPCRs expressed in specific subsets of nociceptive sensory neurons. *Cell* 106**,** 619-632.

Ellis, A., and Bennett, D.L. (2013). Neuroinflammation and the generation of neuropathic pain. *Br J Anaesth* 111**,** 26-37.

Fan, X., and Kurgan, L. (2015). Comprehensive overview and assessment of computational prediction of microRNA targets in animals. *Brief Bioinform* 16**,** 780-794.

Francia, N., Cirulli, F., Chiarotti, F., Antonelli, A., Aloe, L., and Alleva, E. (2006). Spatial memory deficits in middle-aged mice correlate with lower exploratory activity and a subordinate status: role of hippocampal neurotrophins. *Eur J Neurosci* 23**,** 711-728.

Freeman, G.J., Long, A.J., Iwai, Y., Bourque, K., Chernova, T., Nishimura, H., Fitz, L.J., Malenkovich, N., Okazaki, T., Byrne, M.C., Horton, H.F., Fouser, L., Carter, L., Ling, V., Bowman, M.R., Carreno, B.M., Collins, M., Wood, C.R., and Honjo, T. (2000). Engagement of the PD-1 immunoinhibitory receptor by a novel B7 family member leads to negative regulation of lymphocyte activation. *J Exp Med* 192**,** 1027-1034.

Gabriely, G., Wurdinger, T., Kesari, S., Esau, C.C., Burchard, J., Linsley, P.S., and Krichevsky, A.M. (2008). MicroRNA 21 promotes glioma invasion by targeting matrix metalloproteinase regulators. *Mol Cell Biol* 28**,** 5369-5380.

Genda, Y., Arai, M., Ishikawa, M., Tanaka, S., Okabe, T., and Sakamoto, A. (2013). microRNA changes in the dorsal horn of the spinal cord of rats with chronic constriction injury: A TaqMan(R) Low Density Array study. *Int J Mol Med* 31**,** 129-137.

Gustorff, B., Dorner, T., Likar, R., Grisold, W., Lawrence, K., Schwarz, F., and Rieder, A. (2008). Prevalence of self-reported neuropathic pain and impact on quality of life: a prospective representative survey. *Acta Anaesthesiol Scand* 52**,** 132-136.

Hargreaves, K., Dubner, R., Brown, F., Flores, C., and Joris, J. (1988). A new and sensitive method for measuring thermal nociception in cutaneous hyperalgesia. *Pain* 32**,** 77-88.

Hess, G.D., Joseph, J.A., and Roth, G.S. (1981). Effect of age on sensitivity to pain and brain opiate receptors. *Neurobiol Aging* 2**,** 49-55.

Heyn, J., Luchting, B., Hinske, L.C., Hubner, M., Azad, S.C., and Kreth, S. (2016). miR-124a and miR-155 enhance differentiation of regulatory T cells in patients with neuropathic pain. *J Neuroinflammation* 13**,** 248.

Hoeijmakers, J.G., Faber, C.G., Merkies, I.S., and Waxman, S.G. (2015). Painful peripheral neuropathy and sodium channel mutations. *Neurosci Lett* 596**,** 51-59.

Hoffman, Y., Dahary, D., Bublik, D.R., Oren, M., and Pilpel, Y. (2013). The majority of endogenous microRNA targets within Alu elements avoid the microRNA machinery. *Bioinformatics* 29**,** 894-902.

Hori, N., Narita, M., Yamashita, A., Horiuchi, H., Hamada, Y., Kondo, T., Watanabe, M., Igarashi, K., Kawata, M., Shibasaki, M., Yamazaki, M., Kuzumaki, N., Inada, E., Ochiya, T., Iseki, M., Mori, T., and Narita, M. (2016). Changes in the expression of IL-6-Mediated MicroRNAs in the dorsal root ganglion under neuropathic pain in mice. *Synapse* 70**,** 317-324.

Hsu, S.D., Lin, F.M., Wu, W.Y., Liang, C., Huang, W.C., Chan, W.L., Tsai, W.T., Chen, G.Z., Lee, C.J., Chiu, C.M., Chien, C.H., Wu, M.C., Huang, C.Y., Tsou, A.P., and Huang, H.D. (2011). miRTarBase: a database curates experimentally validated microRNA-target interactions. *Nucleic Acids Res* 39**,** D163-169.

Huang, S.Y., Sung, C.S., Chen, W.F., Chen, C.H., Feng, C.W., Yang, S.N., Hung, H.C., Chen, N.F., Lin, P.R., Chen, S.C., Wang, H.M., Chu, T.H., Tai, M.H., and Wen, Z.H. (2015). Involvement of phosphatase and tensin homolog deleted from chromosome 10 in rodent model of neuropathic pain. *J Neuroinflammation* 12**,** 59.

Ibrahim, T., Nekolla, S.G., Langwieser, N., Rischpler, C., Groha, P., Laugwitz, K.L., and Schwaiger, M. (2012). Simultaneous positron emission tomography/magnetic resonance imaging identifies sustained regional abnormalities in cardiac metabolism and function in stress-induced transient midventricular ballooning syndrome: a variant of Takotsubo cardiomyopathy. *Circulation* 126**,** e324-326.

Iliopoulos, D., Kavousanaki, M., Ioannou, M., Boumpas, D., and Verginis, P. (2011). The negative costimulatory molecule PD-1 modulates the balance between immunity and tolerance via miR-21. *Eur J Immunol* 41**,** 1754-1763.

Ingoglia, N.A., and Jalloh, B. (2016). 76nt RNAs are transported axonally into regenerating axons and growth cones. What are they doing there? *Neural Regeneration Research* 11**,** 390-391.

Iorio, M.V., and Croce, C.M. (2012). MicroRNA dysregulation in cancer: diagnostics, monitoring and therapeutics. A comprehensive review. *EMBO Mol Med* 4**,** 143-159.

Jaggi, A.S., Jain, V., and Singh, N. (2011). Animal models of neuropathic pain. *Fundam Clin Pharmacol* 25**,** 1-28.

Jain, R., Jain, S., Raison, C.L., and Maletic, V. (2011). Painful diabetic neuropathy is more than pain alone: examining the role of anxiety and depression as mediators and complicators. *Curr Diab Rep* 11**,** 275-284.

Jensen, T.S., and Finnerup, N.B. (2014). Allodynia and hyperalgesia in neuropathic pain: clinical manifestations and mechanisms. *Lancet Neurol* 13**,** 924-935.

Jopling, C.L., Yi, M., Lancaster, A.M., Lemon, S.M., and Sarnow, P. (2005). Modulation of hepatitis C virus RNA abundance by a liver-specific MicroRNA. *Science* 309**,** 1577-1581.

Julius, D., and Basbaum, A.I. (2001). Molecular mechanisms of nociception. *Nature* 413**,** 203-210.

Katz, M.G., Fargnoli, A.S., Kendle, A.P., Hajjar, R.J., and Bridges, C.R. (2016). The role of microRNAs in cardiac development and regenerative capacity. *Am J Physiol Heart Circ Physiol* 310**,** H528-541.

Kawasaki, Y., Xu, Z.Z., Wang, X., Park, J.Y., Zhuang, Z.Y., Tan, P.H., Gao, Y.J., Roy, K., Corfas, G., Lo, E.H., and Ji, R.R. (2008). Distinct roles of matrix metalloproteases in the early- and late-phase development of neuropathic pain. *Nat Med* 14**,** 331-336.

Kim, S.H., and Chung, J.M. (1992). An experimental model for peripheral neuropathy produced by segmental spinal nerve ligation in the rat. *Pain* 50**,** 355-363.

Kuner, R. (2010). Central mechanisms of pathological pain. *Nat Med* 16**,** 1258-1266.

Kuner, R., and Flor, H. (2016). Structural plasticity and reorganisation in chronic pain. *Nat Rev Neurosci* 18**,** 20-30.

Kusuda, R., Cadetti, F., Ravanelli, M.I., Sousa, T.A., Zanon, S., De Lucca, F.L., and Lucas, G. (2011). Differential expression of microRNAs in mouse pain models. *Mol Pain* 7**,** 17.

Lamberty, Y., and Gower, A.J. (1993). Spatial processing and emotionality in aged NMRI mice: a multivariate analysis. *Physiol Behav* 54**,** 339-343.

Latchman, Y., Wood, C.R., Chernova, T., Chaudhary, D., Borde, M., Chernova, I., Iwai, Y., Long, A.J., Brown, J.A., Nunes, R., Greenfield, E.A., Bourque, K., Boussiotis, V.A., Carter, L.L., Carreno, B.M., Malenkovich, N., Nishimura, H., Okazaki, T., Honjo, T., Sharpe, A.H., and Freeman, G.J. (2001). PD-L2 is a second ligand for PD-1 and inhibits T cell activation. *Nat Immunol* 2**,** 261-268.

Lawrie, C.H., Soneji, S., Marafioti, T., Cooper, C.D., Palazzo, S., Paterson, J.C., Cattan, H., Enver, T., Mager, R., Boultwood, J., Wainscoat, J.S., and Hatton, C.S. (2007). MicroRNA expression distinguishes between germinal center B cell-like and activated B cell-like subtypes of diffuse large B cell lymphoma. *Int J Cancer* 121**,** 1156-1161.

Lee, R.C., Feinbaum, R.L., and Ambros, V. (1993). The C. elegans heterochronic gene lin-4 encodes small RNAs with antisense complementarity to lin-14. *Cell* 75**,** 843-854.

Leffler, A., Linte, R.M., Nau, C., Reeh, P., and Babes, A. (2007). A high-threshold heat-activated channel in cultured rat dorsal root ganglion neurons resembles TRPV2 and is blocked by gadolinium. *Eur J Neurosci* 26**,** 12-22.

Leinders, M., Doppler, K., Klein, T., Deckart, M., Rittner, H., Sommer, C., and Uceyler, N. (2016a). Increased cutaneous miR-let-7d expression correlates with small nerve fiber pathology in patients with fibromyalgia syndrome. *Pain* 157**,** 2493-2503.

Leinders, M., Üçeyler, N., Pritchard, R.A., Sommer, C., and Sorkin, L.S. (2016b). Increased miR-132-3p expression is associated with chronic neuropathic pain. *Exp Neurol* 283**,** 276-286.

Leite-Almeida, H., Almeida-Torres, L., Mesquita, A.R., Pertovaara, A., Sousa, N., Cerqueira, J.J., and Almeida, A. (2009). The impact of age on emotional and cognitive behaviours triggered by experimental neuropathy in rats. *Pain* 144**,** 57-65.

Lemmer, S., Schiesser, P., Geis, C., Sommer, C., Vanegas, H., and Uceyler, N. (2015). Enhanced spinal neuronal responses as a mechanism for the increased nociceptive sensitivity of interleukin-4 deficient mice. *Exp Neurol* 271**,** 198-204.

Lewis, B.P., Burge, C.B., and Bartel, D.P. (2005). Conserved seed pairing, often flanked by adenosines, indicates that thousands of human genes are microRNA targets. *Cell* 120**,** 15-20.

Li, Z., and Rana, T.M. (2014). Therapeutic targeting of microRNAs: current status and future challenges. *Nat Rev Drug Discov* 13**,** 622-638.

Lin, C.R., Chen, K.H., Yang, C.H., Huang, H.W., and Sheen-Chen, S.M. (2014). Intrathecal miR-183 delivery suppresses mechanical allodynia in mononeuropathic rats. *Eur J Neurosci* 39**,** 1682-1689.
Liu, C., Kelnar, K., Liu, B., Chen, X., Calhoun-Davis, T., Li, H., Patrawala, L., Yan, H., Jeter, C., Honorio, S., Wiggins, J.F., Bader, A.G., Fagin, R., Brown, D., and Tang, D.G. (2011a). The microRNA miR-34a inhibits prostate cancer stem cells and metastasis by directly repressing CD44. *Nat Med* 17**,** 211-215.
Liu, R., Zhang, C., Hu, Z., Li, G., Wang, C., Yang, C., Huang, D., Chen, X., Zhang, H., Zhuang, R., Deng, T., Liu, H., Yin, J., Wang, S., Zen, K., Ba, Y., and Zhang, C.Y. (2011b). A five-microRNA signature identified from genome-wide serum microRNA expression profiling serves as a fingerprint for gastric cancer diagnosis. *Eur J Cancer* 47**,** 784-791.
Liu, T., Van Rooijen, N., and Tracey, D.J. (2000). Depletion of macrophages reduces axonal degeneration and hyperalgesia following nerve injury. *Pain* 86**,** 25-32.
Lumpkin, E.A., and Caterina, M.J. (2007). Mechanisms of sensory transduction in the skin. *Nature* 445**,** 858-865.
Ma, W., and Quirion, R. (2006). Increased calcitonin gene-related peptide in neuroma and invading macrophages is involved in the up-regulation of interleukin-6 and thermal hyperalgesia in a rat model of mononeuropathy. *J Neurochem* 98**,** 180-192.
Martirosyan, N.L., Carotenuto, A., Patel, A.A., Kalani, M.Y., Yagmurlu, K., Lemole, G.M., Jr., Preul, M.C., and Theodore, N. (2016). The Role of microRNA Markers in the Diagnosis, Treatment, and Outcome Prediction of Spinal Cord Injury. *Front Surg* 3**,** 56.
Mcdonald, M.K., Tian, Y., Qureshi, R.A., Gormley, M., Ertel, A., Gao, R., Aradillas Lopez, E., Alexander, G.M., Sacan, A., Fortina, P., and Ajit, S.K. (2014). Functional significance of macrophage-derived exosomes in inflammation and pain. *Pain* 155**,** 1527-1539.
Mcmanus, D.D., and Freedman, J.E. (2015). MicroRNAs in platelet function and cardiovascular disease. *Nat Rev Cardiol* 12**,** 711-717.
Mirzaei, V., Manaheji, H., Keramati, K., Maghsodi, N., and Zaringhalam, J. (2008). Comparison of pain behavior responses in two peripheral neuropathic models (SNI, CCI) in rat. *Physiology and Pharmacology* 11**,** 276-281.
Moalem, G., Xu, K., and Yu, L. (2004). T lymphocytes play a role in neuropathic pain following peripheral nerve injury in rats. *Neuroscience* 129**,** 767-777.
Mogil, J.S., Wilson, S.G., Bon, K., Lee, S.E., Chung, K., Raber, P., Pieper, J.O., Hain, H.S., Belknap, J.K., Hubert, L., Elmer, G.I., Chung, J.M., and Devor, M. (1999). Heritability of nociception I: responses of 11 inbred mouse strains on 12 measures of nociception. *Pain* 80**,** 67-82.
Moriarty, O., Mcguire, B.E., and Finn, D.P. (2011). The effect of pain on cognitive function: a review of clinical and preclinical research. *Prog Neurobiol* 93**,** 385-404.
Morris, R. (1984). Developments of a water-maze procedure for studying spatial learning in the rat. *J Neurosci Methods* 11**,** 47-60.
Namer, B., Schick, M., Kleggetveit, I.P., Orstavik, K., Schmidt, R., Jorum, E., Torebjork, E., Handwerker, H., and Schmelz, M. (2015). Differential sensitization of silent nociceptors to low pH stimulation by prostaglandin E2 in human volunteers. *Eur J Pain* 19**,** 159-166.
Napoli, I., Noon, L.A., Ribeiro, S., Kerai, A.P., Parrinello, S., Rosenberg, L.H., Collins, M.J., Harrisingh, M.C., White, I.J., Woodhoo, A., and Lloyd, A.C. (2012). A

central role for the ERK-signaling pathway in controlling Schwann cell plasticity and peripheral nerve regeneration in vivo. *Neuron* 73**,** 729-742.
Niederberger, E., Kynast, K., Lotsch, J., and Geisslinger, G. (2011). MicroRNAs as new players in the pain game. *Pain* 152**,** 1455-1458.
O'leary, T.P., Gunn, R.K., and Brown, R.E. (2013). What are we measuring when we test strain differences in anxiety in mice? *Behav Genet* 43**,** 34-50.
Orlova, I.A., Alexander, G.M., Qureshi, R.A., Sacan, A., Graziano, A., Barrett, J.E., Schwartzman, R.J., and Ajit, S.K. (2011). MicroRNA modulation in complex regional pain syndrome. *J Transl Med* 9**,** 195.
Ostrand-Rosenberg, S., Horn, L.A., and Haile, S.T. (2014). The programmed death-1 immune-suppressive pathway: barrier to antitumor immunity. *J Immunol* 193**,** 3835-3841.
Palazzo, E., Luongo, L., Guida, F., Marabese, I., Romano, R., Iannotta, M., Rossi, F., D'aniello, A., Stella, L., Marmo, F., Usiello, A., De Bartolomeis, A., Maione, S., and De Novellis, V. (2016). D-Aspartate drinking solution alleviates pain and cognitive impairment in neuropathic mice. *Amino Acids* 48**,** 1553-1567.
Pasquinelli, A.E., Reinhart, B.J., Slack, F., Martindale, M.Q., Kuroda, M.I., Maller, B., Hayward, D.C., Ball, E.E., Degnan, B., Muller, P., Spring, J., Srinivasan, A., Fishman, M., Finnerty, J., Corbo, J., Levine, M., Leahy, P., Davidson, E., and Ruvkun, G. (2000). Conservation of the sequence and temporal expression of let-7 heterochronic regulatory RNA. *Nature* 408**,** 86-89.
Pellow, S., Chopin, P., File, S.E., and Briley, M. (1985). Validation of open:closed arm entries in an elevated plus-maze as a measure of anxiety in the rat. *J Neurosci Methods* 14**,** 149-167.
Porsolt, R.D., Bertin, A., and Jalfre, M. (1977). Behavioral despair in mice: a primary screening test for antidepressants. *Arch Int Pharmacodyn Ther* 229**,** 327-336.
Prut, L., and Belzung, C. (2003). The open field as a paradigm to measure the effects of drugs on anxiety-like behaviors: a review. *Eur J Pharmacol* 463**,** 3-33.
Ramos, A. (2008). Animal models of anxiety: do I need multiple tests? *Trends Pharmacol Sci* 29**,** 493-498.
Rupaimoole, R., and Slack, F.J. (2017). MicroRNA therapeutics: towards a new era for the management of cancer and other diseases. *Nat Rev Drug Discov* 16**,** 203-222.
Saito, T., and Saetrom, P. (2012). Target gene expression levels and competition between transfected and endogenous microRNAs are strong confounding factors in microRNA high-throughput experiments. *Silence* 3**,** 3.
Sakai, A., and Suzuki, H. (2013). Nerve injury-induced upregulation of miR-21 in the primary sensory neurons contributes to neuropathic pain in rats. *Biochem Biophys Res Commun* 435**,** 176-181.
Schoeniger-Skinner, D.K., Ledeboer, A., Frank, M.G., Milligan, E.D., Poole, S., Martin, D., Maier, S.F., and Watkins, L.R. (2007). Interleukin-6 mediates low-threshold mechanical allodynia induced by intrathecal HIV-1 envelope glycoprotein gp120. *Brain Behav Immun* 21**,** 660-667.
Seltzer, Z., Dubner, R., and Shir, Y. (1990). A novel behavioral model of neuropathic pain disorders produced in rats by partial sciatic nerve injury. *Pain* 43**,** 205-218.
Sheedy, F.J. (2015). Turning 21: Induction of miR-21 as a Key Switch in the Inflammatory Response. *Front Immunol* 6**,** 19.
Snider, W.D., and Mcmahon, S.B. (1998). Tackling pain at the source: new ideas about nociceptors. *Neuron* 20**,** 629-632.

Soreq, H., and Wolf, Y. (2011). NeurimmiRs: microRNAs in the neuroimmune interface. *Trends Mol Med* 17**,** 548-555.
Strickland, I.T., Richards, L., Holmes, F.E., Wynick, D., Uney, J.B., and Wong, L.F. (2011). Axotomy-induced miR-21 promotes axon growth in adult dorsal root ganglion neurons. *PLoS One* 6**,** e23423.
Sun, S., Chen, D., Lin, F., Chen, M., Yu, H., Hou, L., and Li, C. (2016). Role of interleukin-4, the chemokine CCL3 and its receptor CCR5 in neuropathic pain. *Mol Immunol* 77**,** 184-192.
Treede, R.D., Jensen, T.S., Campbell, J.N., Cruccu, G., Dostrovsky, J.O., Griffin, J.W., Hansson, P., Hughes, R., Nurmikko, T., and Serra, J. (2008). Neuropathic pain: redefinition and a grading system for clinical and research purposes. *Neurology* 70**,** 1630-1635.
Turner, M.D., Nedjai, B., Hurst, T., and Pennington, D.J. (2014). Cytokines and chemokines: At the crossroads of cell signalling and inflammatory disease. *Biochim Biophys Acta* 1843**,** 2563-2582.
Tutar, Y. (2014). miRNA and cancer; computational and experimental approaches. *Curr Pharm Biotechnol* 15**,** 429.
Üçeyler, N., Biko, L., Hose, D., Hofmann, L., and Sommer, C. (2016). Comprehensive and differential long-term characterization of the alpha-galactosidase A deficient mouse model of Fabry disease focusing on the sensory system and pain development. *Mol Pain* 12.
Üçeyler, N., Göbel, K., Meuth, S.G., Ortler, S., Stoll, G., Sommer, C., Wiendl, H., and Kleinschnitz, C. (2010). Deficiency of the negative immune regulator B7-H1 enhances inflammation and neuropathic pain after chronic constriction injury of mouse sciatic nerve. *Exp Neurol* 222**,** 153-160.
Üçeyler, N., Topuzoğlu, T., Schiesser, P., Hahnenkamp, S., and Sommer, C. (2011). IL-4 deficiency is associated with mechanical hypersensitivity in mice. *PLoS One* 6**,** e28205.
Usoskin, D., Furlan, A., Islam, S., Abdo, H., Lonnerberg, P., Lou, D., Hjerling-Leffler, J., Haeggstrom, J., Kharchenko, O., Kharchenko, P.V., Linnarsson, S., and Ernfors, P. (2015). Unbiased classification of sensory neuron types by large-scale single-cell RNA sequencing. *Nat Neurosci* 18**,** 145-153.
Van Hecke, O., Austin, S.K., Khan, R.A., Smith, B.H., and Torrance, N. (2014). Neuropathic pain in the general population: a systematic review of epidemiological studies. *Pain* 155**,** 654-662.
Van Rooij, E., Purcell, A.L., and Levin, A.A. (2012). Developing microRNA therapeutics. *Circ Res* 110**,** 496-507.
Volinia, S., Calin, G.A., Liu, C.G., Ambs, S., Cimmino, A., Petrocca, F., Visone, R., Iorio, M., Roldo, C., Ferracin, M., Prueitt, R.L., Yanaihara, N., Lanza, G., Scarpa, A., Vecchione, A., Negrini, M., Harris, C.C., and Croce, C.M. (2006). A microRNA expression signature of human solid tumors defines cancer gene targets. *Proc Natl Acad Sci U S A* 103**,** 2257-2261.
Wanet, A., Tacheny, A., Arnould, T., and Renard, P. (2012). miR-212/132 expression and functions: within and beyond the neuronal compartment. *Nucleic Acids Res* 40**,** 4742-4753.
Wiggins, J.F., Ruffino, L., Kelnar, K., Omotola, M., Patrawala, L., Brown, D., and Bader, A.G. (2010). Development of a lung cancer therapeutic based on the tumor suppressor microRNA-34. *Cancer Res* 70**,** 5923-5930.
Wilson, S.G., and Mogil, J.S. (2001). Measuring pain in the (knockout) mouse: big challenges in a small mammal. *Behav Brain Res* 125**,** 65-73.

Woolf, C.J. (2011). Central sensitization: implications for the diagnosis and treatment of pain. *Pain* 152**,** S2-15.
Wu, D., Raafat, M., Pak, E., Hammond, S., and Murashov, A.K. (2011). MicroRNA machinery responds to peripheral nerve lesion in an injury-regulated pattern. *Neuroscience* 190**,** 386-397.
Xu, Y., Zhang, X., Pu, S., Wu, J., Lv, Y., and Du, D. (2014). Circulating microRNA expression profile: a novel potential predictor for chronic nervous lesions. *Acta Biochim Biophys Sin (Shanghai)* 46**,** 942-949.
Yalcin, I., Barthas, F., and Barrot, M. (2014). Emotional consequences of neuropathic pain: insight from preclinical studies. *Neurosci Biobehav Rev* 47**,** 154-164.
Yezierski, R.P. (2012). The effects of age on pain sensitivity: preclinical studies. *Pain Med* 13 Suppl 2**,** S27-36.
Yu, B., Zhou, S., Qian, T., Wang, Y., Ding, F., and Gu, X. (2011). Altered microRNA expression following sciatic nerve resection in dorsal root ganglia of rats. *Acta Biochim Biophys Sin (Shanghai)* 43**,** 909-915.
Zhao, J., Lee, M.C., Momin, A., Cendan, C.M., Shepherd, S.T., Baker, M.D., Asante, C., Bee, L., Bethry, A., Perkins, J.R., Nassar, M.A., Abrahamsen, B., Dickenson, A., Cobb, B.S., Merkenschlager, M., and Wood, J.N. (2010). Small RNAs control sodium channel expression, nociceptor excitability, and pain thresholds. *J Neurosci* 30**,** 10860-10871.

8 Appendices

8.1 Technical equipment

Analog Vortex Mixer	VWR, Radnor, USA
Biosphere Filter Tips	Sarstedt, Nuernbrecht, Germany
Balance 440-47	Kern AG, Frankfurt am Main, Germany
CCD camera	Visitron Systems, Tuchheim Germany
Centrifuges	
Centrifuge 5417R	Eppendorf, Hamburg, Germany
Rotina 420R	Hettich, Tuttlingen, Germany
Spectrafuge 3-1810	Neolab, Heidelberg, Germany
Clips	B. Braun, Melsungen, Germany
Combitips advanced 0,5 ml	Eppendorf, Hamburg, Germany
Cryostat CM 3050	Leica, Wetzlar, Germany
Falcon tubes (15 ml, 50 ml)	Greiner Bio One GmbH, Frickenhausen, Germany
Freezer comfort -20˚C	Liebherr, Biberach, Germany
Freezer TSX Series -80˚C	Thermo Scientific, Waltham, USA
Hargreaves apparatus	Ugo Basile Inc., Comerio, Italy
Heating plate	Medax, Neumünster, Germany
Homogenizer Polytron PT 1600	Kinematika AG, Luzern, Schweiz
MicroAmp® fast 96-well reaction plate	Applied Biosystems, Darmstadt, Germany
MicroAmp® adhesive film	Applied Biosystems, Darmstadt, Germany
Microscopes	
Axiophot 2	Zeiss, Oberkochen, Germany
BH2	Olympus, Hamburg, Germany
Stemi 2000	Zeiss, Oberkochen, Germany
Multipipette stream	Eppendorf, Hamburg, Germany
NanoPhotometer Pearl®	Implen, Munich, Germany
Needle 27G	B. Braun, Melsungen, Germany
Objectslides superfrost	Langenbrinck, Teningen, Germany
Optical adhesive covers	Langenbrinck, Teningen, Germany
PCR Tubes 0,2 ml, 1,5 ml	Eppendorf, Hamburg, Germany
Parafilm® M	Bemis Company Inc, Oshkosh, USA

PapPen	Sigma-Aldrich, St. Louis, USA
Pipettes	
Research plus	Eppendorf, Hamburg, Germany
Pipetman	Gilson, Bad Camberg, Germany
Software	
Anymaze version 4.99m	Stoelting, Wood Dale, USA
Image J free software version 1.51f	National Institute of Health, USA
Office 2010	Microsoft, Redmond, USA
GraphPad Prism, version 5.03	GraphPad Software, San Diego, USA
Spot version 5.2	Spot Software BV, Amsterdam, Netherlands
SPSS IBM version 23	IBM, Ehningen, Germany
Surgical Blades	B. Braun, Melsungen, Germany
Surgical cutlery	FST, Heidelberg, Germany
Suture	
7-0 Prolene	Ethicon, Somerville, USA
6/0 Silkam	B. Braun, Melsungen, Germany
5-0 Vicryl	Ethicon, Somerville, USA
Syringes 1 ml, 5 ml, 10 ml	BD, Franklin Lakes, USA
Thermocycler	
Step One Plus Real Time PCR	Applied Biosystems, Darmstadt, Germany
Peqstar	Peqlab, Erlangen, Germany
Primus 96	Peqlab, Erlangen, Germany
Tissue-Tek® Cryomold	Sakura, Staufen, Germany
Von Frey filaments	Stoelting, Wood Dale, USA

8.2 Reagents

Agarose	Roth, Karlsruhe, Germany
Avidin/Biotin blocking kit	Vector Laboratories, Burlingame, USA
Bovine serum albumine	Sigma-Aldrich, München, Germany
cDNA Synthesis kit ll	Exiqon, Vedbaek, Denmark
Diaminobenzidine (DAB) Peroxidase Substrate Kit SK-4100	Vector Laboratories, Burlingame, USA
Diethylpyrocarbonate (DEPC)	Sigma-Aldrich, München, Germany

DNeasy blood&tissue kit	Qiagen, Hilden, Germany
Ethanol	Sigma-Aldrich, München, Germany
Ethylenediaminetetraacetic acid (EDTA)	Merck, Darmstadt, Germany
ExiLENT SYBR® Green master mix	Exiqon, Vedbaek, Denmark
Dream Taq HS Green master Mix	Life Technologies, Carlsbad, USA
Hematoxylin	Sigma-Aldrich, München, Germany
i-Fect™	Neuromics, Edina, USA
In vivo inhibitor (miR-21-5p)	Exiqon, Vedbaek, Denmark
Isoflurane CP®	CP Pharma, Burgdorf, Germany
Kapa2G fast PCR Kit	Kapa Biosystems, Wilmington, USA
Leukocyte purification kit	Norgen biotek corp., Thorold, Canada
miRNeasy Micro Kit	Qiagen, Hilden, Germany
2-Mercaptoethanol	Carl Roth, Karlsruhe, Germany
2-Methylbutane	Carl Roth, Karlsruhe, Germany
Nuclease free water	Applied Biosystems, Darmstadt, Germany
O.C.T Medium	Sakura, Staufen, Germany
ROX Reference Dye	Invitrogen, Carlsbad, USA
Sodium chloride solution	Merck, Darmstadt, Germany
TagMan Universal PCR master Mix	Applied Biosystems, Darmstadt, Germany
TaqMan Micro RNA RT Kit	Applied Biosystems, Darmstadt, Germany
Vitro-Clud®	Langenbrinck, Teningen, Germany

8.3 Buffers and solutions

DEPC-H_2O	0.01 % DEPC Dissolve in distilled water, autoclave
PBS (1x)	137 mM NaCl 2.7 mM KCL 1.5 mM KH_2PO_4 8.1 mM Na_2PO_4 pH 7.4

8.4 Primer sequences for genotyping

B7-H1

WT FW 5`AGAACGGGAGCTGGACCTGCTTGCGTTAG3`

REV 5`ATTGACTTTCAGCGTGATTCGCTT GTAG3`

KO Neo 5`TTC TAT CGC CTT CTT GAC GAG TTC TCC TG 3`

8.5 Primer used for qRT-PCR

Table 1: miCURY LNA™ Universal microRNA PCR Primer (Exiqon, Vedbaek, Denmark)

Gene	Sequence 5´-3´	Product number
miR-21-5p	UAGCUUAUCAGACUGAUGUUGA	204230
Sno202	GCTGTACTGACTTGATGAAAGTA CTTTTGAACCCTTTTCCATCTGAT G	206999
U6	not specified	308013
Snord65	not specified	203910
U1A1	not specified	203909
5S	not specified	203906
Snord110	not specified	203912
RNU5G	not specified	203908

Table 2: TaqMan qRT-PCR Assays (Applied Biosystems, Darmstadt, Germany)

Gene	Sequence 5'-3'	Assay ID
18sRNA	not specified	Hs99999901_s1
Cd274	not specified	Mm03048248_m1
SnoRNA202	GCTGTACTGACTTGATGAAAGTA CTTTTGAACCCTTTTCCATCTGAT G	001232
SnoRNA234	CTTTTGGAACTGAATCTAAGTGAT TTAACAAAAATTCGTCACTACCAC TGAGA	001234

8.6 Antibodies used in immunohistochemistry

Table 3: Primary antibodies

Reactivity	Host	Company	Catalog #	Dilution	Fixation / Additives
CD 3	Rat	Serotec	MCA1477	1:100	Acetone
CD11b	Rat	Serotec	MCA 711	1:250	Acetone

Table 4: Secondary antibodies

Reactivity	Host	Company	Catalog #	Dilution	Fixation / Additives
Biotinylated Anti-Rat IgG, mouse adsorbed	Rabbit	Vector	BA-4001	1:200	Acetone

9 Abbreviations

AGO2	Argonaute 2
AMPA	α-amino-3-hydroxy-5-methyl-4-isoxazolepropionic acid
B7-H1	B7 homolog 1
BSA	bovine serum albumin
C57BL/6	C57 black 6
CCD	charge-coupled device
CCI	chronic constriction injury
CD	cluster of differentiation
cDNA	complementary deoxyribonucleic acid
CGRP	calcitonin-gene related peptide
CNS	central nervous system
CRPS	complex regional pain syndrome
DAB	diaminobenzidine
DGCR8	DiGeorge syndrome critical region 8
DNA	deoxyribonucleic acid
DRG	dorsal root ganglion
EPM	elevated plus maze
ERK	extracellular signal-regulated kinases
FST	forced-swim test
GDNF	glial cell-derived neurotrophic factor
HCV	hepatitis C virus
IASP	International Association for the Study of Pain
IBM	International Business Machines
IFN-γ	interferon
IL	interleukin
ko	knock out
LDB	light-dark box
let-7	lethal-7
LNA	locked nucleic acid
MAP	mitogen-activated protein
MET	MET proto-pncogene, receptor tyrosine kinase
miRNA, miR	micro ribonucleic acid
mRNA	messenger ribonucleic acid

MTI	micro ribonucleic acid–target interactions
MWM	Morris water maze
Nav1.7	voltage-gated sodium channel 1.7
ncRNA	non coding ribonucleic acid
NGF	nerve growth factor
OCT	optimum cutting temperature
NMDA	N-methyl-D-aspartate
OF	open field
PBS	phosphate-buffered saline
PCR	polymerase chain reaction
PD-1	programmed cell death protein 1
PDCD4	programmed cell death 4
PD-L	programmed death-ligand
PNS	peripheral nervous system
pre-miRNA	precursor micro ribonucleic acid
pri-miRNA	primary micro ribonucleic acid
PSL	partial sciatic nerve ligation
PT	probe trail
PTEN	phosphatase and tensin homolog
p value	probability value
qRT-PCR	quantitative real-time-polymerase chain reaction
RECK	reversion inducing cysteine rich protein with kazal motifs
RISC	ribonucleic acid-induced silencing complex
RNA	ribonucleic acid
SCN9A	sodium voltage-gated channel alpha subunit 9
Scr	mismatch control
SNI	spared nerve injury
SNL	sciatic nerve ligation
SPSS	statistical package of the social sciences
STAT5	signal transducer and activator of transcription 5
TCR	T cell receptor
TIMP3	tissue inhibitor of metalloproteinase 3
TNF	tumor necrosis factor-alpha
TRBP	transactivating response ribonucleic acid-binding protein 2

Tris	tris(hydroxymethyl)-aminomethan
TrkA	tropomyosin receptor kinase A
TRPM8	transient receptor potential cation channel subfamily M member 8
TRPV	transient receptor potential cation channel subfamily V member
UTR	3' untranslated region
VEGF	vascular endothelial growth factor
WBC	white blood cells
WT	wildtype

10 List of Figures and Tables

11 Curriculum vitae

12 Publications

Peer reviewed journals; original articles

Karl F, Grießhammer A, Üçeyler N and Sommer C (2017) Differential impact of miR-21 on pain and associated affective and cognitive behavior after spared nerve injury in B7-H1 ko mouse. Front Mol Neurosci 10:219. doi: 10.3389/fnmol.2017.00219.

Hofmann L, **Karl F**, Sommer C, Üçeyler N (2017) Affective and cognitive behavior in the alpha-galactosidase A deficient mouse model of Fabry disease. PLoS One 12, e0180601.

Lüningschrör P, Beyenech B, Dombert B, Heimann P, Perez L, Slotta C, Thau N, Rüdt von Collenberg C, **Karl F**, Damme M, Horowitz A, Maystadt I, Füchtbauer A, Füchtbauer E, Jablonka S, Blum R, Üçeyler N, Petri S, Kaltschmidt B, Jahn R, Kaltschmidt C, Sendtner M (2017) Plekhg5-regulated autophagy of synaptic vesicles reveals a new pathogenic mechanism in motoneuron disease. Nat Comm. 2017, in press.

Scherzer S, Krol E, Kreuzer I, Kruse J, **Karl F**, von Rüden M, Escalante-Perez M, Müller T, Rennenberg H, Al-Rasheid KA, Neher E, Hedrich R (2013) The Dionaea muscipula ammonium channel DmAMT1 provides NH4+ uptake associated with Venus flytrap's prey digestion. Curr Biol. 23:1649-57.

Poster presentations at international conferences

Karl F, Grießhammer A, Üçeyler N, Sommer C (2017) The role of miR-21 in neuropathic pain and affective behavior after peripheral nerve injury in B7-H1 knockout mice. 6th International Congress on Neuropathic Pain, Gothenburg, Sweden

Karl F, Üçeyler N, Sommer C (2016) The role of miR-21 in neuropathic pain and affective behavior after peripheral nerve injury in B7-H1 knockout mice. 11th international symposium EUREKA, Würzburg, Germany

Karl F, Üçeyler N, Sommer C (2016) The role of miR-21 in neuropathic pain and affective behavior after peripheral nerve injury in B7-H1 knockout mice. 16th World Congress on Pain, Yokohama, Japan

13 Danksagung

An dieser Stelle möchte ich mich besonders bei Frau Prof. Dr. Claudia Sommer für die Betreuung meiner Thesis und die Möglichkeit der Durchführung in ihrer Arbeitsgruppe bedanken.

Mein größter Dank gilt Frau Prof. Dr. Nurcan Üçeyler, deren stetige Unterstützung während meiner Arbeit von unschätzbarem Wert ist.

Bei Frau Dr. Ana Eulalio und Herrn Prof. Dr. Thomas Dandekar möchte ich mich für die wissenschaftlichen Ratschläge und die konstruktive Kritik während der jährlichen Meetings recht herzlich bedanken. Weiterhin möchte ich mich bei Prof. Dr. Ulrike Holzgrabe für die Übernahme des Prüfungsvorsitzes bedanken.

Meinen Labor- und Bürokollegen Lukas Hofmann, Thomas Klein, Luisa Kress und Dr. Dimitar Evdokimov möchte ich für die sehr schöne Zeit im Büro, sowie für die tolle Arbeitsatmosphäre danken.

Mein besonderer Dank gilt Frau Lydia Biko, die mich bei allen tierexperimentellen Versuchen unterstützte und mir stets mit Rat und Tat aus ihrem großen Erfahrungsschatz zur Seite stand.

Ein großes Dankeschön geht an Frau Helga Brünner, die mich bei allen tierexperimentellen Fragen und der aufwändigen Bürokratie stets unterstützte, und an das Team der Tierhaltung Neurologie für die gute Pflege der Mäuse.

Bei den technischen Mitarbeiterinnen der AG Sommer / Üçeyler, Frau Sonja Mildner, Frau Barbara Dekant, Frau Katharina Meder bedanke ich mich recht herzlich für die Hilfsbereitschaft und die experimentelle Unterstützung.

Nicht zuletzt bedanke ich mich bei meiner Familie, meinem Freund und allen Freunden, die mich jederzeit unterstützt haben.